geologica acta

Citation: Shahab, M., Ali, L., Alshehri, F., 2025. An Integrated Remote Sensing, Petrographic, and Mineralogical Techniques for Mapping of Marble Deposits in the Vicinity of the Ophiolite Sequence in North Pakistan. Geologica Acta, 23.4, 1-22.

Online ISSN: 1696-5728 DOI: 10.1344/GeologicaActa2025.23.4

An Integrated Remote Sensing, Petrographic, and Mineralogical Techniques for Mapping of Marble Deposits in the Vicinity of the Ophiolite Sequence in North Pakistan

Muhammad Shahab[1,2,3] **Liaqat Ali**[1,2] **Fahad Alshehri**[3]

[1]**National Centre of Excellence in Geology, University of Peshawar**
Peshawar 25130, Pakistan

[2]**GIS and Space Application in Geosciences (GSAG) Lab, National Centre of GIS and Space Application (NCGSA)**
Islamabad 44000, Pakistan

[3]**Abdullah Alrushaid Chair for Earth Science Remote Sensing Research, Geology and Geophysics Department, College of Science, King Saud University**
P.O. Box 2455, Riyadh 11451, Saudi Arabia
Correspondence: shahabgeo07@gmail.com

ABSTRACT

Marble, a high-pressure and high-temperature metamorphic rock primarily composed of calcium carbonate ($CaCO_3$) and calcium magnesium carbonate ($CaMgCO_3$), has been utilized extensively by ancient civilizations for various architectural purposes globally. The expansion of marble production during the 19th century facilitated its widespread use, with major quarries emerging in various regions, notably China, India, Italy, and Turkey. Despite its historical significance and economic importance, mapping and identifying marble deposits in remote and inaccessible areas remain challenging. This study presents an integrated approach utilizing advanced remote sensing techniques for mapping carbonate lithologies in the Northwest Mohmand District, Khyber Pakhtunkhwa, Pakistan. By employing Advanced Spaceborne Thermal Emission and Reflection Radiometry (ASTER) imaging coupled with Iterative Adaptive Reweighted Regression (IARR), Principal Component Analysis (PCA), Minimum Noise Fraction (MNF) and Spectral Angle Mapper (SAM) classification techniques, we processed and analysed the ASTER images using the Environment for Visualizing Images (ENVI) software. Subsequently, Geographic Information Systems (GIS), ArcMap, and ArcScene software were used for spatial analysis and model generation. Validation of the results was conducted through extensive fieldwork, X-Ray Diffraction (XRD), and petrographic analysis. The XRD and petrographic data corroborated the findings derived from the classified ASTER imagery, confirming the presence of significant concentrations of dolomite and calcite, which are indicative of carbonate deposits. The integration of these techniques underscores the efficacy of remote sensing as a viable tool for identifying and mapping mineralized zones in remote locations.

The findings of this study have significant implications for Pakistan's marble industry, particularly in Khyber Pakhtunkhwa, Punjab, and Baluchistan, where an estimated 300 million tons of marble reserves exist. Leveraging remote sensing techniques, this research contributes to the delineation of valuable marble resources and facilitates recommendations for targeted exploration activities in the Mohmand area and beyond.

KEYWORDS **Ophiolites. Marble. ASTER image. Remote sensing. Pakistan.**

INTRODUCTION

Marbles are formed when carbonatite rocks recrystallize at high pressures and temperatures in a specific zone (Vagenas *et al.*, 2003). Carbonatite, an igneous rock composed mainly of carbonate minerals, is classified by the IUGS based on its mineral composition, with carbonate minerals making up more than 50% of its modal percentage (Hay, 1989). Subtypes include calcite carbonatite (dominated by calcite), with sövite and alvikite variations based on grain size (Woolley *et al.*, 1991). Ferro-carbonatite, which is rich in iron carbonate minerals, lacks a precise definition but is suggested for iron-rich cases with unknown modal mineralogy (von Eckermann, 1948). Magnesium-rich varieties were once called "beforsite" but are now termed dolomite or magnesio-carbonatite (Vuorinen, 2005). Natro-carbonatite, a rare type found in Oldoinyo Lengai, Tanzania, consists primarily of nyerereite and gregoryite with a chemical composition of [$(Na, K)_2CO_3$] (Dawson, 1962). Depending on the mineralogy, the major types of marble can be either calcitic ($CaCo_3$) or dolomitic $(CaMgCo_3)_6$ (Anjum *et al.*, 2021; Fahad *et al.*, 2016). The majority of economically valuable resources are calcite-bearing rocks that are widely used in civil construction materials and iron ore smelting, both of which can be used in concrete and asphalt as aggregates for projects around the world; marble is also used as a dimension stone (Koca *et al.*, 2006). The mechanical qualities of concrete mixtures can be enhanced by including marble coarse aggregate (Kore *et al.*, 2020). Apart from stone dimensions, decoration and other purposes, high-purity marbles can be valuable sources of carbonates for use in a wide range of chemical industries, including the production of paper, dyes, paints, tires, plastic, pharmaceuticals, cosmetics, animal feed, lime, soda ash, water purification, and steel (Careddu *et al.*, 2014).

For the identification and exploration of the mineral and ore deposits, Remote Sensing (RS) is a new technology for the collection of surficial information without establishing physical contact with the object based on propagated signals (Guo *et al.*, 2014; Hegab, 2024; Schott, 2007). The RS technique using satellite images, *i.e.* ASTER, can identify and map carbonate formations effectively in a short period before detailed mapping and exploitation. Carbonate formations are differentiated by utilizing the spectral signatures of the main rock-forming mineral which is calcite, to target spatially occurring economic deposits by evaluating their diagnostic absorption signatures (Desoky and Abd El-Dayem, 2019; Rajendran and Nasir, 2014). Advanced Spaceborne Thermal Emission and Reflection Radiometer (ASTER) satellite images was launched in 1999 (Yajima, 2014). ASTER data have better spectral, spatial, and radiometric resolutions than other multispectral data (Mars and Rowan, 2006). The spectral bands of ASTER have been useful in identifying mineral and ore deposits and associated lithologies in the exploration of minerals and ore deposits (Ali, *et al.*, 2023; Ghoneim, *et al.*, 2024; Rajendran and Nasir, 2019). To obtain more accurate results, RS data were integrated with mineralogical data X-Ray Diffraction (XRD) and petrographic results. With this approach, inaccessible areas can be explored and mapped (Crósta *et al.*, 2003; Ninomiya, 2003). ASTER data have better spectral, spatial, and radiometric resolutions than other multispectral data (Hegab and Mousa, 2022; Mars and Rowan, 2006).

Since, the quality of marble for several applications is limited by the presence of various impurities, such as SiO_2, Fe_2O_3, Al_2O_3 and MgO, chemical analysis of marble is required to determine its grade and suitability. Pakistan is one of the top rich countries in marble deposits; 300 million tons of marble reserves are present, and there are more than approximately 1600 active units nationwide, with more than 400 operational units in KP Province (Ur Rehman *et al.*, 2022). Mountainous terrains cover more than 70% of KP and Ex-FATA's area, which is approximately 74,521 square kilometres. The northern part of the province has marble reserves, according to geological surveys, the part of KP, previously called FATA, has 200 million tons, accounting for more than 60% of national marble production. The region contains more than 30 different types of marble based on its composition (Malkani *et al.*, 2017). The primary objective of this research is to explore the distributions of marble deposits in district Mohmand area by using remote sensing techniques and identifying marble quarries based our remote sensing results. The investigation was facilitated through the integration of satellite imagery, which helped us identify the zones for field visits while the petrography, and mineralogical studies validated our remote sensing results. The aim is to identify and map the marble deposits within district Mohmand. This innovative methodology allows for the identification and mapping of potential Marble deposits with greater efficiency than traditional exploration methods, particularly in remote localities like district Mohmand which was unexplored due to remote location and hostile law and order situation. Consequently, the research contributes to the advancement of Marble deposits exploration practices, offering novel insights into the geological context and spatial distribution of the potential marble deposits zones.

Local and Regional Geological Setting

The Indus Suture Zone (ISZ) marks the boundary where the northern edge of the Indian plate meets the Asian landmass. In Pakistan, the two plates Indian and Karakoram are separated by a large rock body known as the Kohistan Island Arc (KIA), which was formed as a result of the subduction of the Tethys Ocean and subsequent collision with the Karakoram Block. (Burg *et al.*, 1998; Jagoutz *et*

al., 2019). In the suture zone and the western hinterland, specific mélange zones, such as Dargai, Kishora, Shergarh, and Nawagi, which are extensions of the ISZ, are found. (Ahmad *et al.*, 2000; DiPietro *et al.*, 2008). The available published literature on the district of Mohmand, including the study area, mostly consists of preliminary investigations. (Kazmi *et al.* 1985; Majid and Shah 1985; Tahirkehli 1979) studied the mélange zones along the MMT exposed at various places, including the study area (Haqqani and Ahmaduddin,2006). This particular geological formation is unique because of its top location over the Malakand slice, as well as the abundance of marble, which is found in significant quantities towards the upper part of the mélange (DiPietro *et al.*, 2008). The study area, as shown in (Fig. 1), is geologically located near Nawagi Mélange, a sub-zone of the ISZ, which lies to the north of the MMT and south of the Kohistan Fault. It is distinguished from other mélanges by its structural position on the Malakand slice and extensive outcrops of Nawagi marble. The dominant lithologies include Marble, schist, and gray to black and green phyllites, while serpentine and talc-carbonate schist occur as subordinate lithologies (DiPietro *et al.*, 2000, 2008).

Geographic Location of the Study Area

Geographically, Mohmand District lies to the north of Peshawar, bordered by the Bajaur district to the north, the Khyber district to the south, the Malakand district to the east, and a lengthy border with Afghanistan to the west (Fig. 2). The recent transition of Mohmand from its prior status as an agency to that of a settled district in 2011 following the FATA merger delineates a significant shift towards mainstream governance. This transition not only reflects a departure from the traditional administrative structure but also underscores a broader move towards integrating these regions within the larger framework of the KP government. Understanding the intricate geographic dynamics of Mohmand District, including its adjacency to Malakand and its placement within the Peshawar division, presents compelling opportunities for miners and mineral exploration companies. The district's transition to

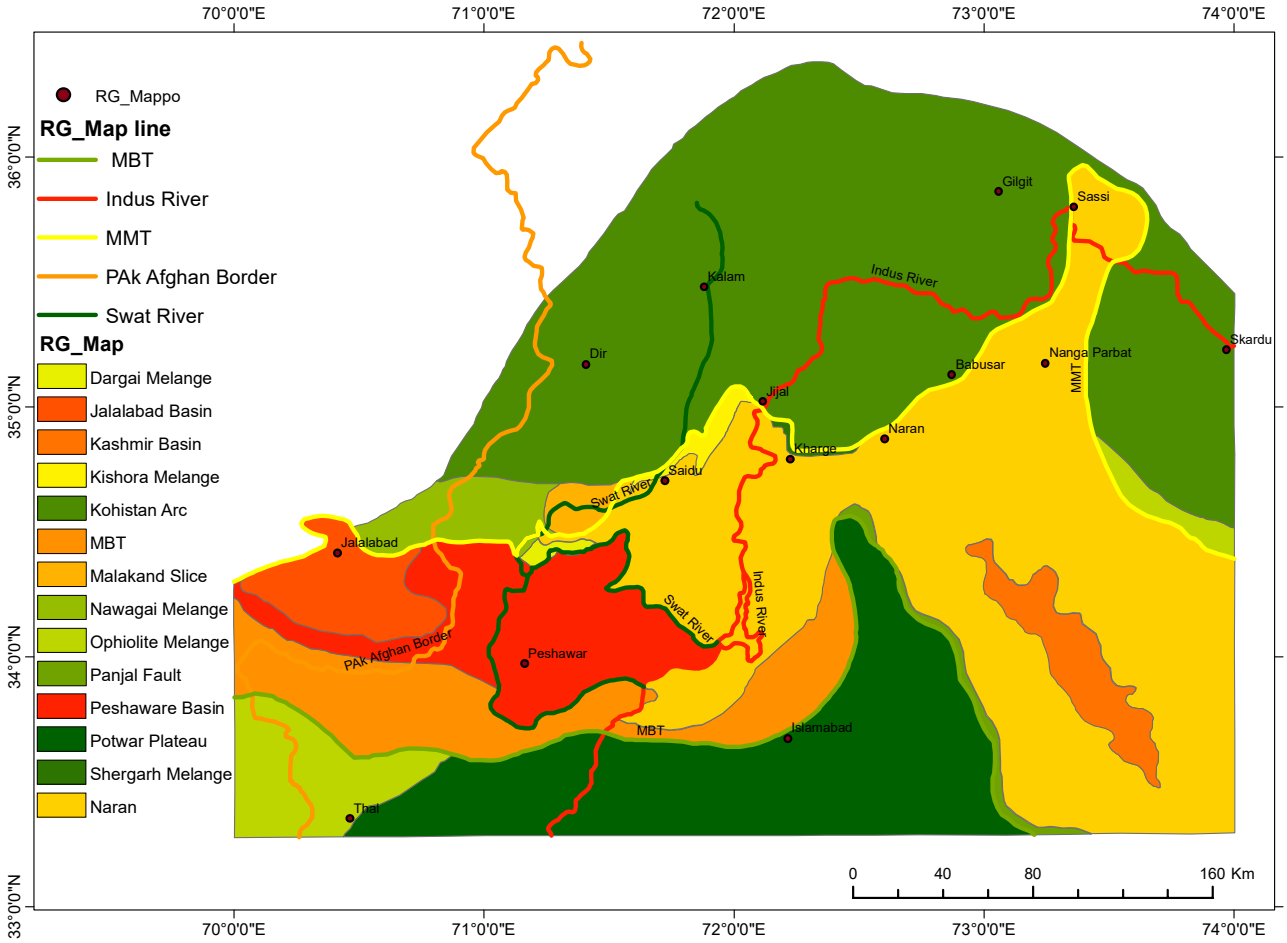

FIGURE 1. Digitized regional geological map of the northern areas of Pakistan showing the major thrusts in Pakistan: main mantle thrust, main boundary thrust and salt range thrust.

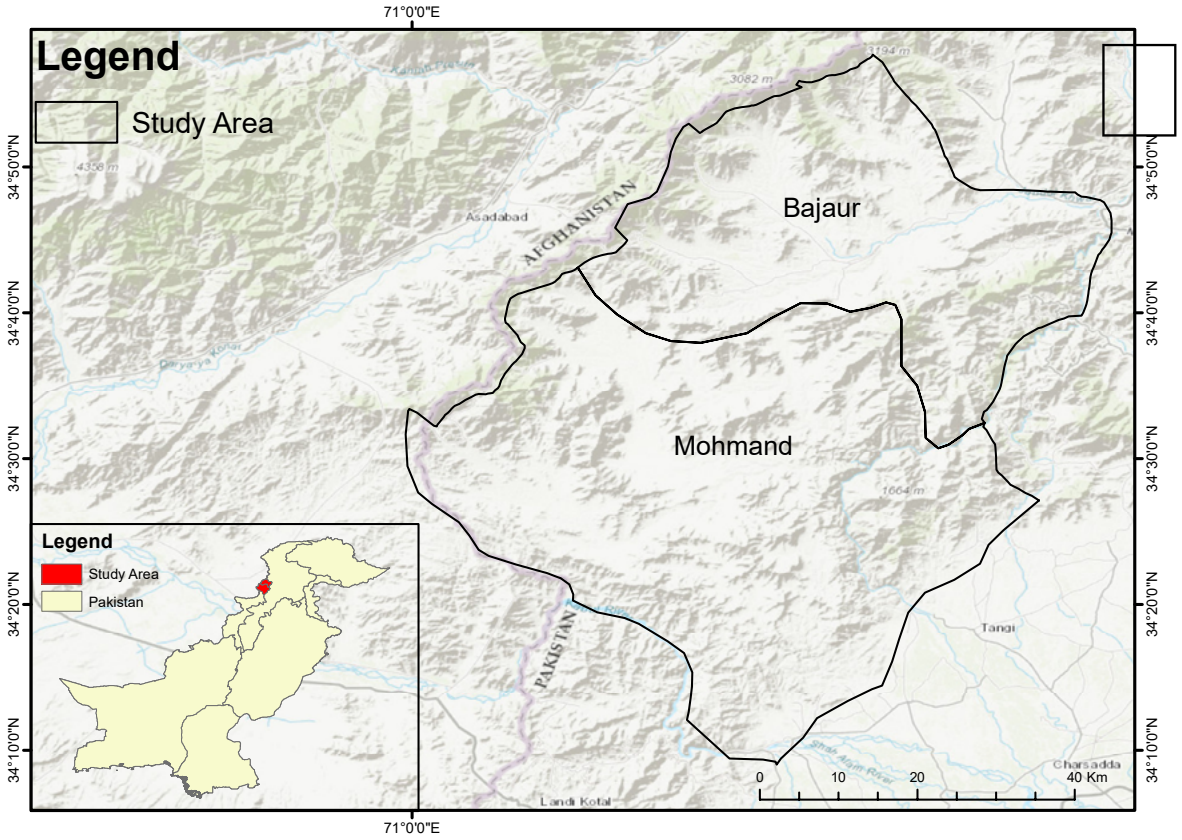

FIGURE 2. Shows the geographic location of the study area; the red line boundaries are showing the Bajaur and Mohmand Districts of Khyber Pakhtunkhwa Pakistan.

a settled administrative unit, coupled with its rich mineral endowments, signifies a conducive environment for mineral exploration and extraction endeavours. This geographical context underscores the potential for economic development and resource utilization within Mohmand, thereby positioning the district as a promising location for mining operations (Ahmad and Khan, 2019; Khan, 2022; Ullah *et al.*, 2024).

MATERIALS AND METHODS

Remote Sensing Data

ASTER, launched by NASA in December 1999, is a research tool equipped with 14 bands, offering spatial resolutions of 15m in the Visible Near-Infrared (VNIR) region, 30m in the Shortwave Infrared (SWIR) region and 90m in the Thermal Infrared (TIR) region. Its wide spectral wavelength ranges of 0.52-0.86, 1.60-2.43, and 8.12-11.65 micrometres in the VNIR, SWIR and TIR regions, respectively, make it particularly advantageous for geological mapping, providing comprehensive data compared to other multispectral instruments (Drusch *et al.*, 2012; Muhammad *et al.*, 2024; Xiong *et al.*, 2011). ASTER data AST_L1T_00303302008061130_20150523133034_105548 of the study area acquired on 2008/03/30 were obtained from the Earth Explorer website (https://earthexplorer.usgs.gov/). Cloud cover, vegetation, and atmospheric correction were carefully considered during image acquisition because these parameters can significantly impact image visualization and interpretation. Metadata examination ensured the availability of all bands for the image. Image processing involved radiometric calibration, band stacking, and environmental correction through Iterative Adaptive Reweighted Regression (IARR) correction. This correction is crucial for mitigating the influence of atmospheric molecules and aerosols on multispectral sensor data (Berk *et al.*, 2009; Yuan and Nui, 2008). Following IARR correction, various analysis methods, such as True Colour Composite (TCC), Band Ratio (BR), Minimum Noise Fraction (MNF), Principal Component Analysis (PCA) and Spectral Angle Mapper (SAM), were applied to discriminate the different lithologies (Al-Nahmi *et al.*, 2017). These techniques are instrumental in identifying and mapping geologic features, particularly carbonate deposits, using remote sensing data. The BR technique is a commonly employed method in remote

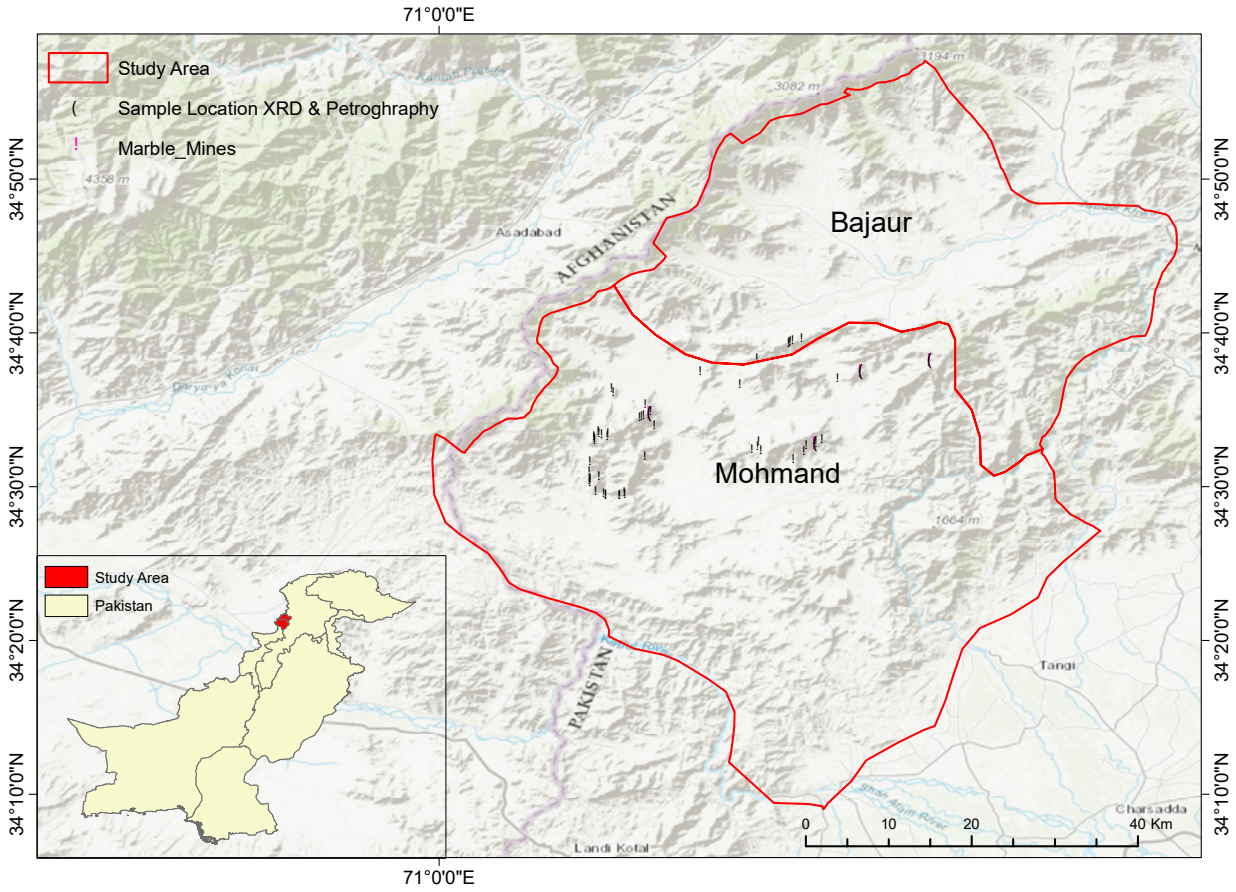

FIGURE 3. Shows the location of the collected samples points in black color points and the pink color is showing the selected points based similar specification of marbles.

sensing for identifying various types of rocks and minerals. This study aimed to utilize the BR technique to differentiate carbonate rocks from other materials (Rasouli Beirami and Tangestani, 2020). The MNF technique is a computational method utilized to identify surface features, including geological patterns, by analysing the spectral reflectance of an image. This study employs the MNF technique to identify different types of carbonate rocks, particularly limestone, using spectral reflectance as a reference for the selected features (Azizi *et al.*, 2010; Ninomiya and Fu, 2016; Ninomiya *et al.*, 2005; Rajendran and Nasir, 2014). PCA is a linear transformation that highlights data with highest variance and minimal correlation and generates uncorrelated spectral bands, thereby reducing noise and redundancy in the data. Using eigenvector analysis as a basis, the Crosta technique focusses on desired spectral properties by choosing particular main components (Carranza and Hale, 2002; Crosta and Moore, 1989; Hegab, 2021). This method has been widely used in mineral exploration using ASTER data to improve mineralogical signatures (Moradpour *et al.*, 2022; Sekandari *et al.*, 2022; Ullah and Li, 2022). SAM rapidly determines how closely an image's spectral signature resembles reference spectra (Hegab, 2021; Malekzadeh, 2009). SAM is a supervised classification method that uses the spectral angle between spectra to identify distinct classes in an image. The spectra are treated as vectors in a multi-dimensional space, with the number of dimensions equal to the number of bands in the image. Reference spectra can also be acquired from pre-existing spectral libraries or field observations (Kruse and Bordman, 2003). The SAM classification method enhances the distinction between rock types by highlighting the specific reflectance characteristics of each lithological unit (Rezaei and Hassani, 2019). This is study follow the scheme shown in (Fig. 5).

Fieldwork

Extensive fieldwork was conducted within the Mohmand district to delineate areas of interest utilizing ASTER images and remote sensing methodologies, ultimately revealing active marble quarries within the region. Thorough investigations were undertaken on the exposed rock formations, with detailed scrutiny

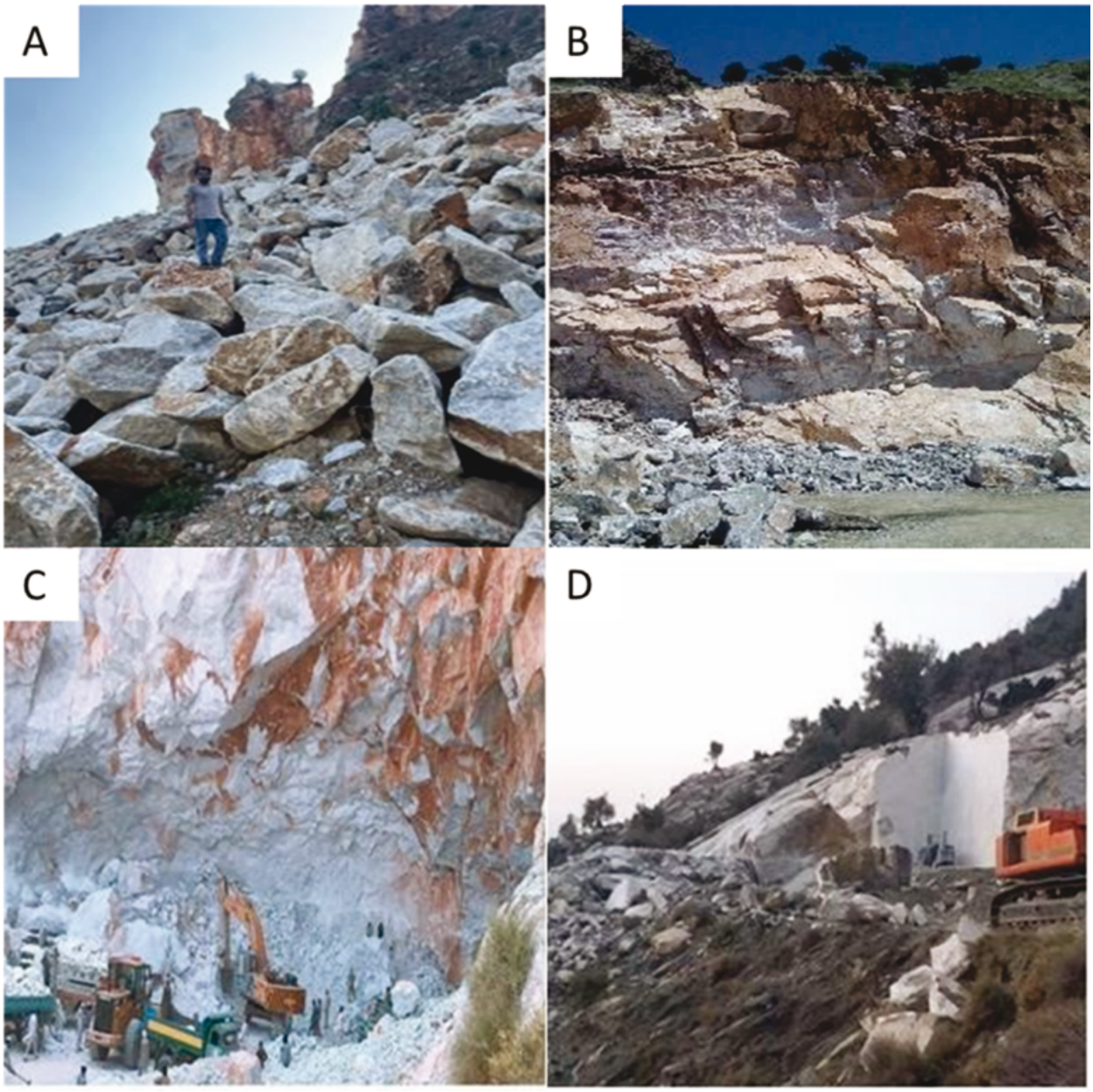

FIGURE 4. Field photograph showing the marble quarries visited in the area.

of outcrops and subsequent collection of samples (Fig. 3) from several marble quarries (Fig. 4). For this research we collected specifically 30 samples, later for XRD and petrography we chose 4 localities which describe the major types of deposits in the region. The collected specimens underwent meticulous processing for petrographic and mineralogical analyses, specifically employing XRD techniques. Locations of all acquired samples was meticulously executed through the utilization of a Geographic Positioning System (GPS) (Fig. 3). Subsequently, these samples were transported to the National Centre of Excellence in Geology (NCEG) Laboratories for further analytical procedures and assessment.

Thin Section Preparation for Petrographic Analysis

Petrographic analysis of the selected samples was conducted at the NCEG. Thin sections were meticulously prepared from the selected samples using a diamond saw, followed by precise polishing with a grinder to facilitate petrographic investigation. The polished specimens were subjected to a drying process at 35ºC on a hot plate, after which they were affixed onto glass surfaces using epoxy

glue. Subsequently, the mounted slabs cut with the help of grinding machine and Polished through applications of silicon carbide abrasive grits ranging from 400 to 1000 microns until the sample thickness was reduced to 30mm.

X-Ray Diffraction (XRD)

XRD serves as a fundamental technique in mineralogical analysis, providing insights into mineral composition without necessitating acid dissolution (Shebl and Hamdy, 2023). Rooted in unit cell measurements, XRD is extensively employed for characterizing crystalline materials and identifying distinct phases. Particularly valuable in discerning crystalline substances such as minerals and inorganic chemicals, XRD analysis facilitates the determination of the crystallization degree and differentiation between mineral phases with identical chemical compositions but differing atomic ordering (Ur Rehman *et al.*, 2022). In geological studies, XRD is widely used for decoding mineral crystal structures. An X-ray diffractometer comprises an X-ray tube, a specimen holder, and a detection mechanism. In a specific experimental scenario, marble powder was subjected to XRD analysis on a Bruker AXS D8 Discover machine calibrated under controlled conditions. The operational settings included an angular range of $2\theta = 5°$ to $80°$ with step increments of 0.020 and a timing rhythm of one-second intervals per step. The X-ray tube was operated at forty-five kV and forty mA, with ambient temperature stabilization at approximately twenty-five degrees Celsius (USGS OFR01-041: X-ray Diffraction Primer, n.d.).

RESULTS

Satellite Image Analysis

Multiple images were pre-processed, and the best of all was considered in terms of visuals and spectral response for analysis. First, the RGB technique was applied to discriminate carbonate lithologies from host lithologies, where RGB b4, b6, and b8 show the highest Optimum Index Factor (OIF) value among the 8 different RGBs, as shown in Table 1. Figure 6 shows carbonate lithologies with yellowish colour due to the reflectance in b4 and b6, while b8 shows absorption features between 2.3 and 2.4μm.

Band Ratio

The BR technique was applied to the stacked package of the VNIR and SWIR using different combinations, and the results demonstrated the demarcation of the targeted minerals. Previously published data were extracted from the 9-band package of ASTER to obtain information about the band combination, and self-imposed bands were also applied based on the spectral reflectance, which revealed better visual information in grayscale and RGB images. The literature reports that spectral index such as (b5 + b6 + b9)/ (b7 + b8) are effective in detecting carbonate rocks (El-Desoky, 2024; Rasouli Beirami and Tangestani, 2020). This research adopts different band ratios and spectral indices from manipulating the ASTER bands, including b5/b4, b4/b3, b4/b5, (b7+b9)/b8 and (b4/b2, b4/b5, b5/b6 in RGB) (Fig. 6). From investigating the results, it is found that b5/b4, b4/b3 and (b7+b9)/b8 contain carbonate rocks in white, while RGB 4/2 4/5 5/6 highlights carbonate lithologies in pinkish colour. Since the typical absorption properties of minerals are found in the VNIR-SWIR range of the electromagnetic spectrum, the band ratios computed from the VNIR and SWIR bands of the ASTER dataset proved particularly effective in differentiating between various minerals. The absorption and reflectance patterns of calcite in the SWIR zone are particularly noteworthy. They show a dip in absorption in band B8 (~2.33μm) and significant reflectance in bands B7 and B9 (~2.26 and 2.4μm, respectively) (Fig. 7). As a result, regions rich in calcite are effectively identified by the band ratio (B7+B9)/B8, which is indicated in (Fig. 7) by brighter white zones. Moreover, RGB 4/2, 4/5, and 5/6 represent carbonate rocks that are reddish pink in colour with high visual acuity.

TABLE 1. Shows the FCC band combinations with their Optimum Index Factor (OIF) values

S. no.	R	G	B	OIF score
1	b2	b3	b8	0.42
2	b2	b3	b9	0.41
3	b2	b8	b9	0.41
4	b3	b8	b9	0.40
5	b2	b3	b7	0.40
6	b4	b6	b8	0.39
7	b1	b2	b8	0.45

Principal Component Analysis (PCA)

PCA played an important role in highlighting the lithological variation, and primary lithological information is represented by the PC2, PC4, PC5, PC7, and PC8 component transformations (Fig. 8). The PCA details reveal the variance of each band in grayscale and show that the carbonate lithologies are black in PC2 and white in PC4, PC5, and PC8 (Fig. 7). The red stars in Figures 8 and 9 indicate the marble quarries in the area visited for sample collection and field validation. A greyscale image can highlight one or two lithological classes by each PC. Consequently, to observe the greatest lithological changes in a single image, RGB composites were created using RGB b1 b2 b3, RGB b2 b4 b6, RGB b4 b6 b8 and RGB b4 b6 b7 from the PCA results, which clearly discriminate among

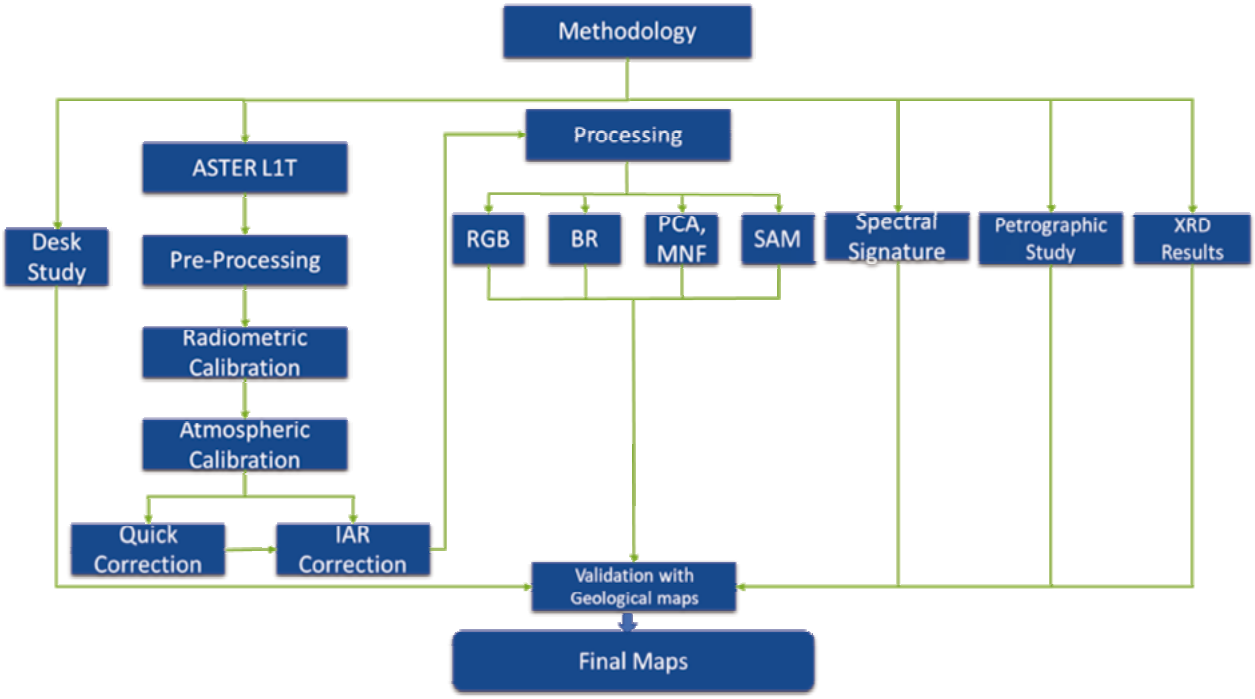

FIGURE 5. Flow chart shows the methodology scheme for the current study, integration of ASTER and its spectral characteristic with the Petrographic and XRD data from field samples.

the lithologies. RGB b1 b2 b3 and RGB b4 b6 b8 show carbonate lithologies in purple, while the vegetation and build-up areas are indicated in green and blue, respectively (Fig. 9). RGB b2 b4 b6 is greenish, and RGB b4 b6 b7 is reddish, as shown in (Fig. 9).

Minimum Noise Fraction (MNF)

MNF is a widely used technique for identifying variations in multispectral data (Alshehri and Shahab, 2025; Rasouli Beirami and Tangestani, 2020). The last two bands of the VNIR, i.e., MNF2 and MNF3, have the greatest variation according to the MNF transformation results (Fig. 10). MNF2, MNF7 and MNF8 visualize the carbonate lithologies in white, while MNF3 and MNF5 discriminate them from the other lithologies in black (Fig. 10). To visualize the maximum lithological variation of the carbonate rocks and better visualize the RGB combination from the MNF VNIR and SWIR bands, RGBs b2 b4 b6, RGB b4 b6 b8, RGB b1 b2 b4 and RGB b1 b2 b6 were created. The RGBs b2 b4 b6 and RGB b4 b6 b8 highlighted the carbonates in a pinkish colour and RGB b1 b2 b4 and RGB b1, b2, b6 highlighted carbonates in a greenish colour (Fig. 11).

Spectral Angle Mapper (SAM)

The spectra of each image pixel and the endmember field are used independently to apply the SAM classification. The visual comparison of the two classifications reveals that, in relation to end-member spectra, the classification based on picture pixels reflects the largest lithological representation. A lithological map of the region showing the surface distribution of the interpreted lithologies is created by performing image classification (Fig. 12) This work uses the spectral characteristics of outcropped lithologies to combine satellite data and field spectrometry data. SAM technology is used for classification. The results of SAM were further processed in Arc scene GIS to create a 3D map of the carbonate lithologies distribution in the area (Fig. 13).

Spectral Signatures of the ASTER Images in Comparison with the USGS Library

The SWIR bands of the ASTER spectral profile cover indicative absorption/reflection features for different minerals. Hence, they play an important role in exploring different minerals exposed on surfaces (Beirami and Tangestani 2020; Fakhari *et al.*, 2019; Rajendran and Nasir 2019a, b; Zaini *et al.*, 2014). False-Color Composite (FCC) b4, b6, and b8 were used for collecting the spectral signatures shown in Figures 14 and 15. The spectral signatures were collected from four different marble quarries and compared with the USGS spectral library for dissimilar carbonate lithologies. The results

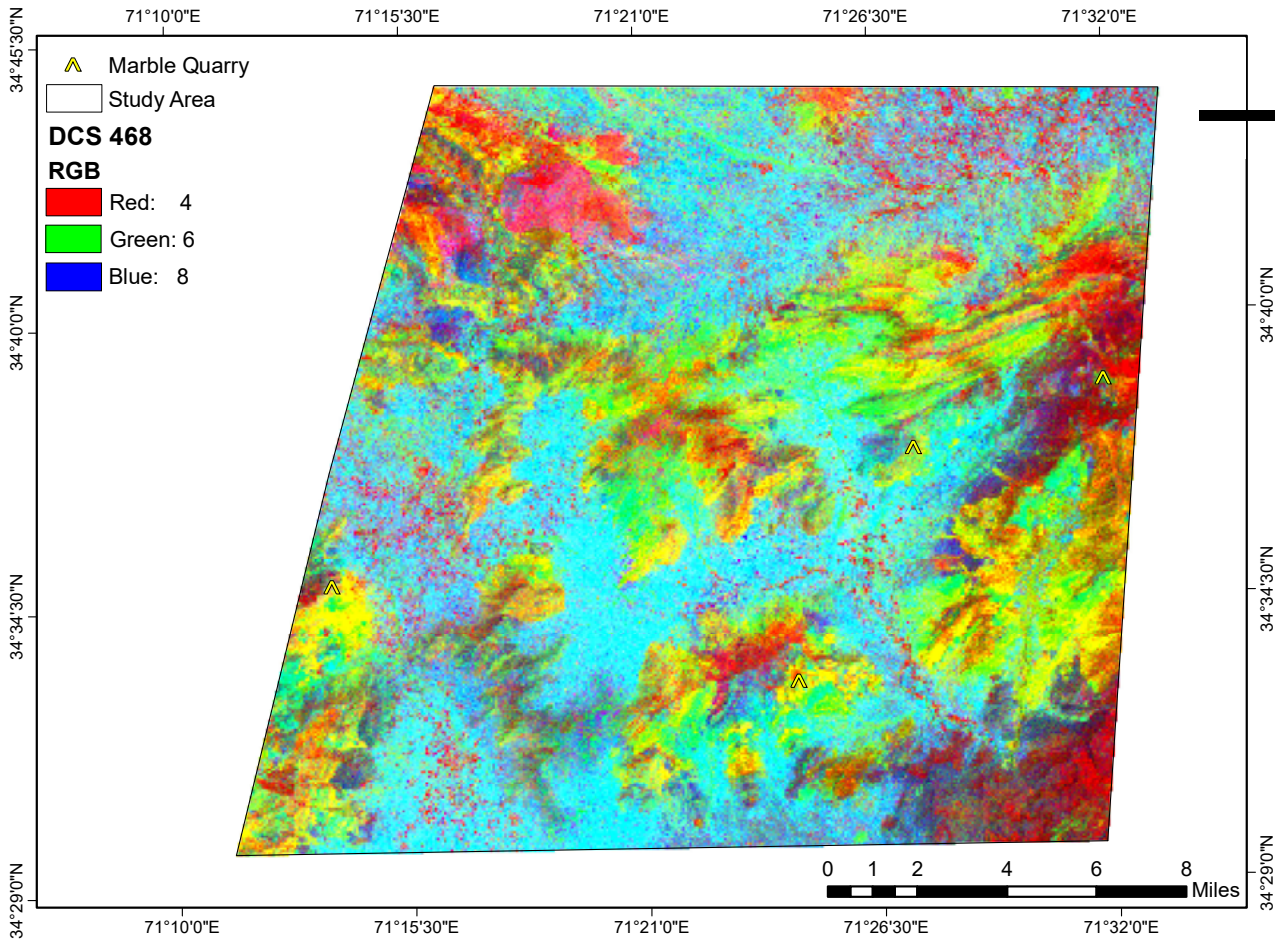

FIGURE 6. Shows the results of band ratios b4, b6, and b8, which clearly highlight the carbonate lithologies in yellow.

revealed the same absorption features after 2.34μm for the carbonate-rich lithologies. Specifically, the absorption feature of CO_3 at a wavelength of 2.34μm is detected within band 8 of the ASTER SWIR regiondataset Top of Form (Beirami and Tangestani, 2020). The point of each collected spectrum was also validated by the SAM results, which confirmed the spectral signature with field work data. Figure 15 also shows location and image of the said quarries.

Petrographic Study

The thin sections were studied in great detail, with the identification of various minerals, such as calcite, quartz, opaque minerals, dolomite, and organic materials, being crucial components of this process. Minerals have different optical properties, and this technique allows us to identify different minerals based on their optical properties. The following photographs are from different queries of marbles from the Mohmand district.

Ziarat Marble (ZM)

The petrographic analysis yielded findings indicating that the Ziarat Marble (ZM) samples (1) and (2) possess distinct mineral compositions. ZM (1) predominantly comprises 94% calcite, with approximately 1% quartz and 5% compacted materials. In contrast, ZM (2) primarily consisted of 95% calcite, approximately 1% quartz, 2% opaque materials, and 2% organic matter (Fig. 16). These results led to the classification of ZM as a fine-grained variety characterized by a grain arrangement demonstrating convex-concave to suture interlocking patterns. The grain boundaries exhibit euhedral to subhedral morphologies, with calcite grains displaying similar orientations. Additionally, localized dissolution phenomena are observed within the material.

K-Moor Marble (KMM)

Petrographic investigation of the KMM, which was derived from a separate quarry, with two distinct samples

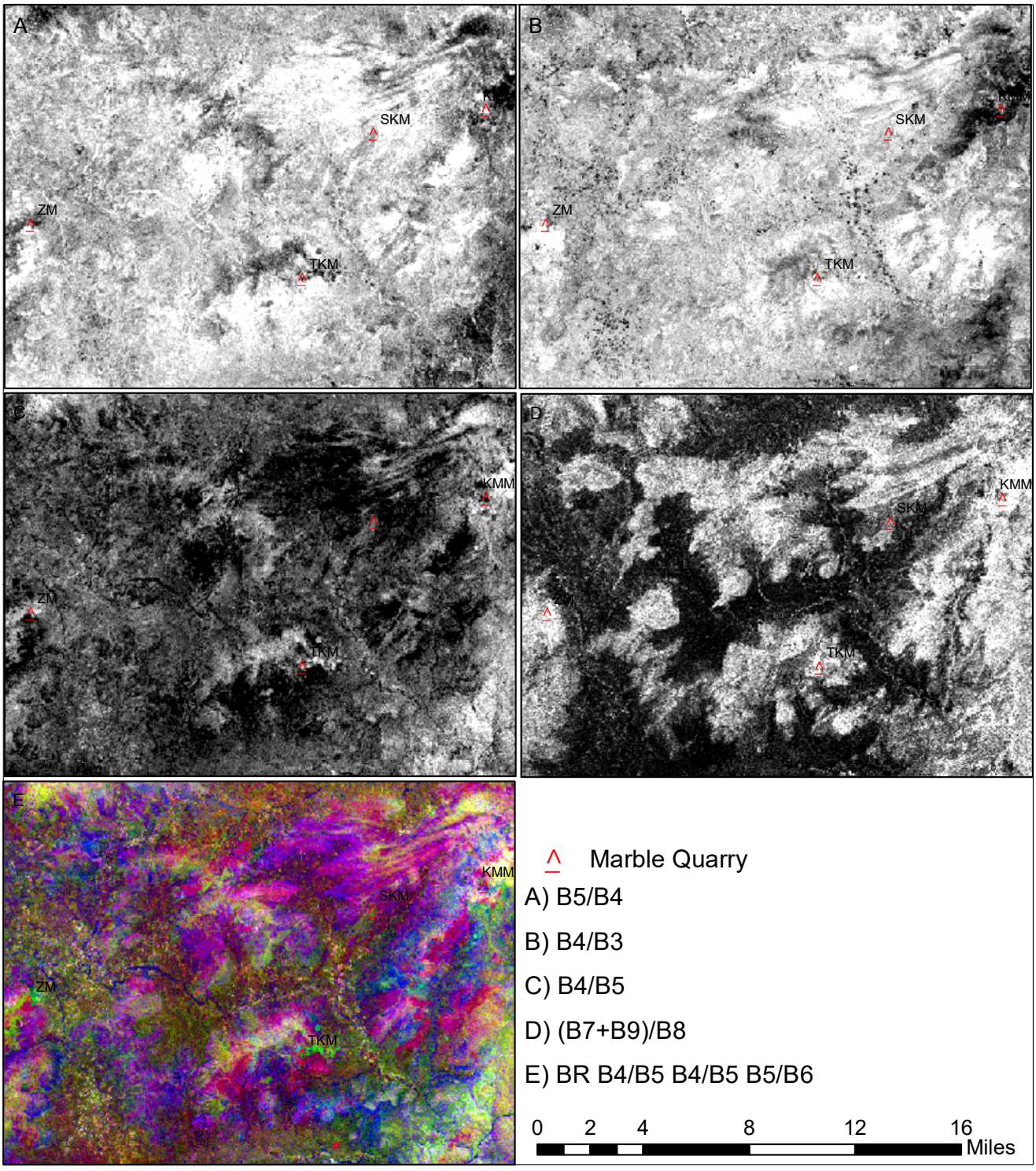

FIGURE 7. Shows different BRs for highlighting the carbonate lithologies in grayscale images and RGB images.

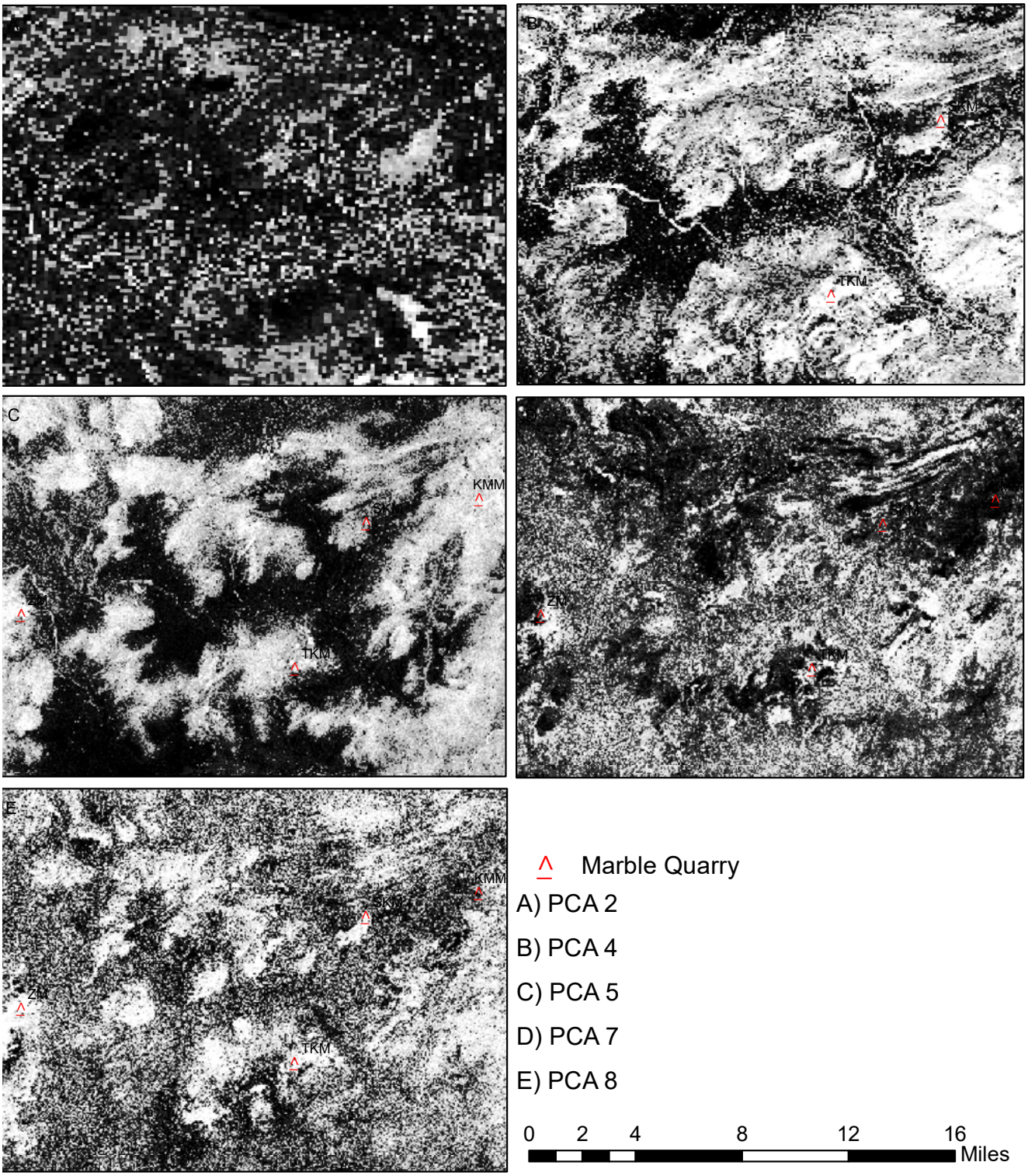

FIGURE 8. Shows the PCA results of PC2, PC4, PC5, PC7 and PC8 in greyscale images using ENVI 5.3.

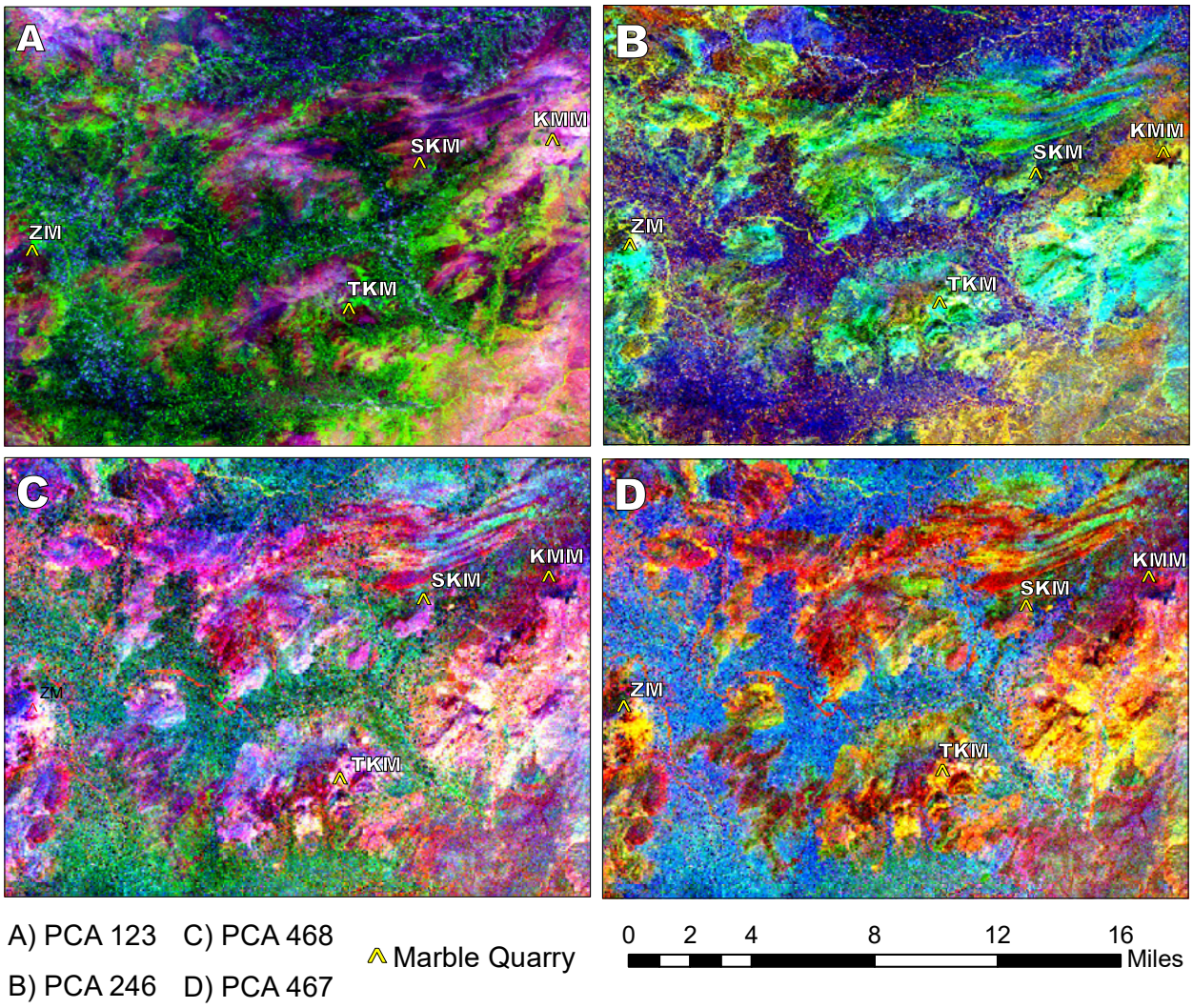

FIGURE 9. Shows PCA b1 b2 b3, PCA b2 b4 b6, PCA b4 b6 b8 and b4 b6 b7, and the red stars are the marble quarries in the area.

labelled S1 and S2. Analysis of S1 revealed a composition predominantly composed of 95% calcite, alongside traces of quartz amounting to less than 1%, approximately 1% opaque materials, and 3% organic matter or unidentified material. Similarly, S2 primarily consisted of 95% calcite, less than 1% quartz, and 3% organic matter (Fig. 17). Petrography was used to elucidate the texture and composition of the KMM. This marble type exhibits a medium to coarse grain structure characterized by planar to sutured or concavo-convex contacts. The mineral grains manifest isometric euhedral to subhedral shapes, indicative of a heteroblastic texture. Microscopic porosity is a prevalent feature within calcite grains, while quartz minerals are notably absent or imperceptible in KMM samples. Furthermore, observations reveal the presence of twinning in calcite crystals, with narrow bands of twinning lamellae denoting metamorphism at relatively low temperatures. The calcite grains distinctly display two sets of cleavages, contributing to the overall mineralogical characterization of KMM.

Sheen Kamar Marble (SKM)

The SKM had a distinctive composition compared to its counterparts from other quarries. Based on the composition classified as medium- to coarse-grained, these marbles feature a range of grain contacts from planar to sutured, reflecting an irregular arrangement with interlocked boundaries indicative of a xeno-blastic texture. The grains exhibit varying morphologies, ranging from subhedral to euhedral. In particular, SKM1 has a composition dominated by 85% calcite, complemented by 10% quartz, 5% opaque constituents and a negligible presence of organic matter. Conversely, SKM2 exhibits a primary composition comprising 91% calcite, 5% quartz, 3% opaque materials and 1% organic matter (Fig. 18).

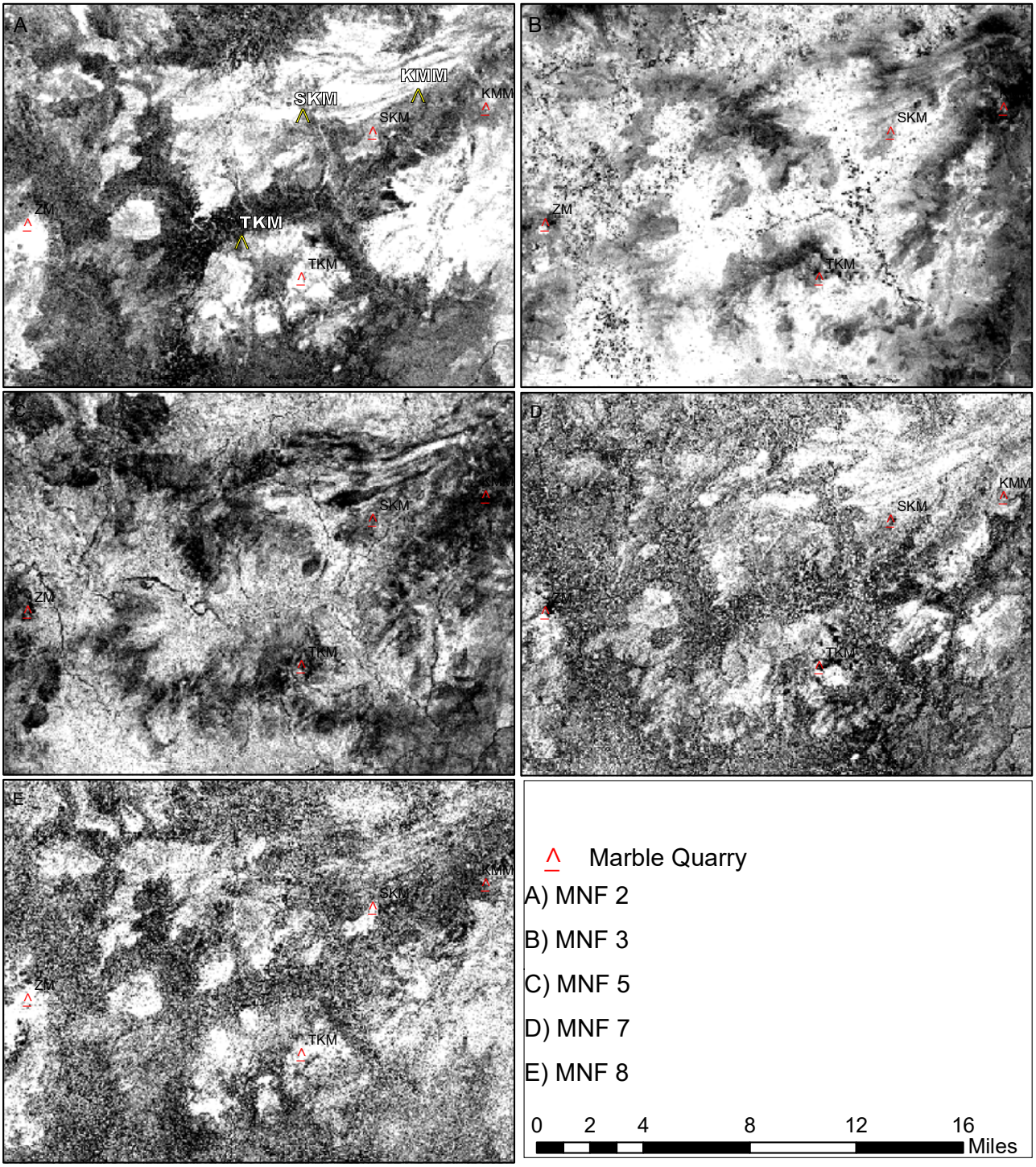

FIGURE 10. Shows the MNF transformations of MNF 2, MNF3, MNF5, MNF7, and MNF8. The red stars indicate marble quarries.

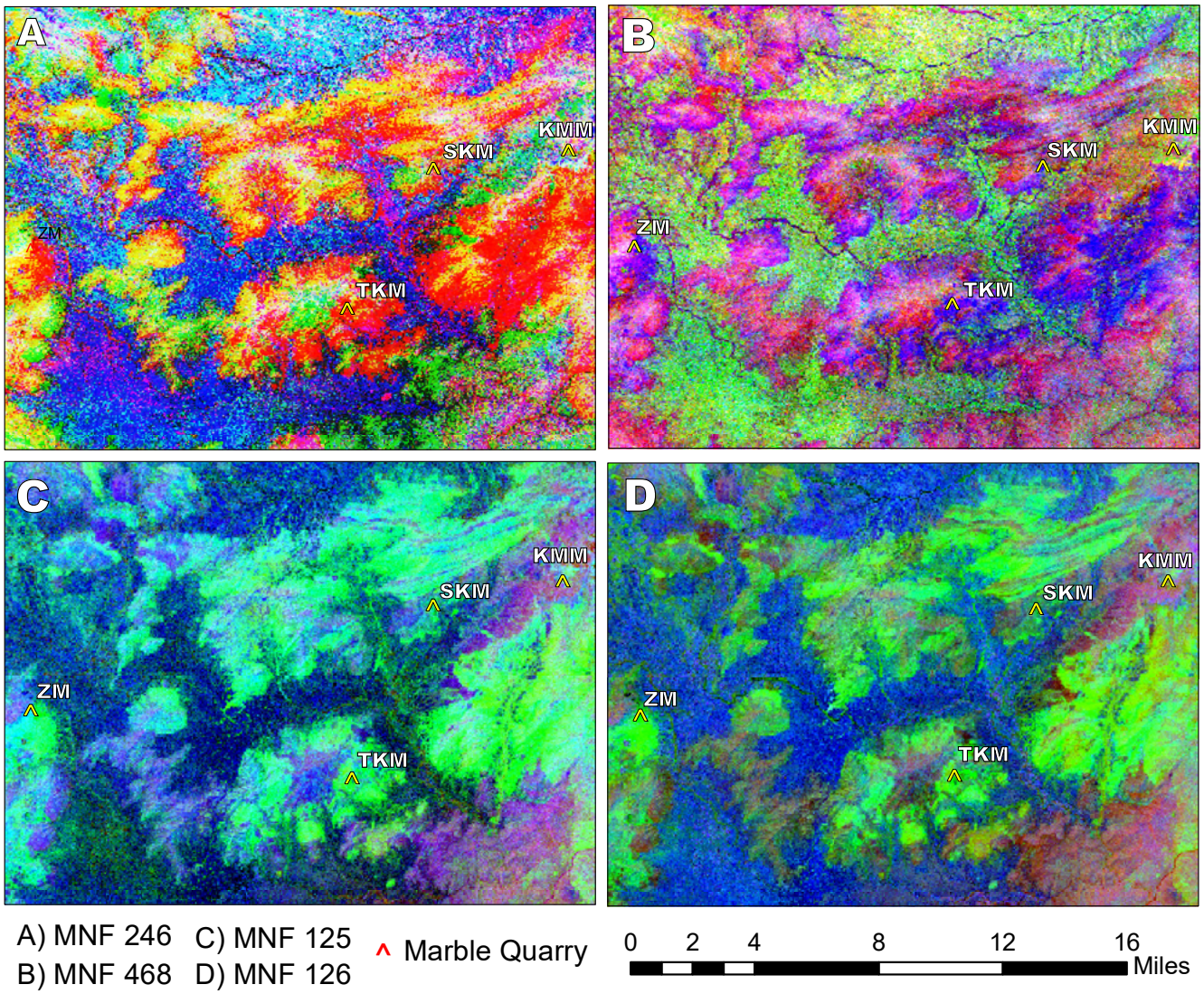

FIGURE 11. Shows the RGBs b2 b4 b6, RGB b4 b6 b8, RGB b1 b2 b4, and RGB b1, b2, b6 from the MNF results.

Tora Khwa Marble (TKM)

The TKM was 96% calcite, 1% quartz, 15% opaque, and 2% organic matter, while the TKM 2 results revealed 91% calcite, 2% quartz, 3% opaque and 4% organic matter. The grains are not fully developed. The grain size varies from medium to coarse. The grains have sutured contacts that overlap with each other. The grains have euhedral to subhedral shapes and heteroblastic textures. Large porphyro-blastics are also observed with dolomite. The quartz minerals are dispersed and small in size. A petrography study of TKM revealed noteworthy compositional attributes, with TKM1 demonstrating a predominant composition of 96% calcite supplemented with 1% quartz, 15% opaque constituents and 2% organic matter. In contrast, TKM2 was primarily composed of 91% calcite, 2% quartz, 3% opaque materials, and 4% organic matter (Fig. 19). The granular structure of TKM displays incomplete development and is characterized by a medium to coarse grain size. Grain interconnectivity is evidenced by sutured contacts with overlapping arrangements. Morphologically, the grains exhibit euhedral to subhedral shapes, indicative of a heteroblastic texture. Notably, large porphyroblasts, accompanied by dolomite, are observed within the matrix. Quartz minerals are dispersed throughout the matrix and present in smaller dimensions.

Mineralogical analysis (XRD) top of the form

In the field of geology, XRD is a widely used analytical technique for identifying and quantifying minerals in rocks and other geological materials (Surko *et al.*, 1999). This technique is particularly useful for identifying and quantifying minerals in complex geological samples, such

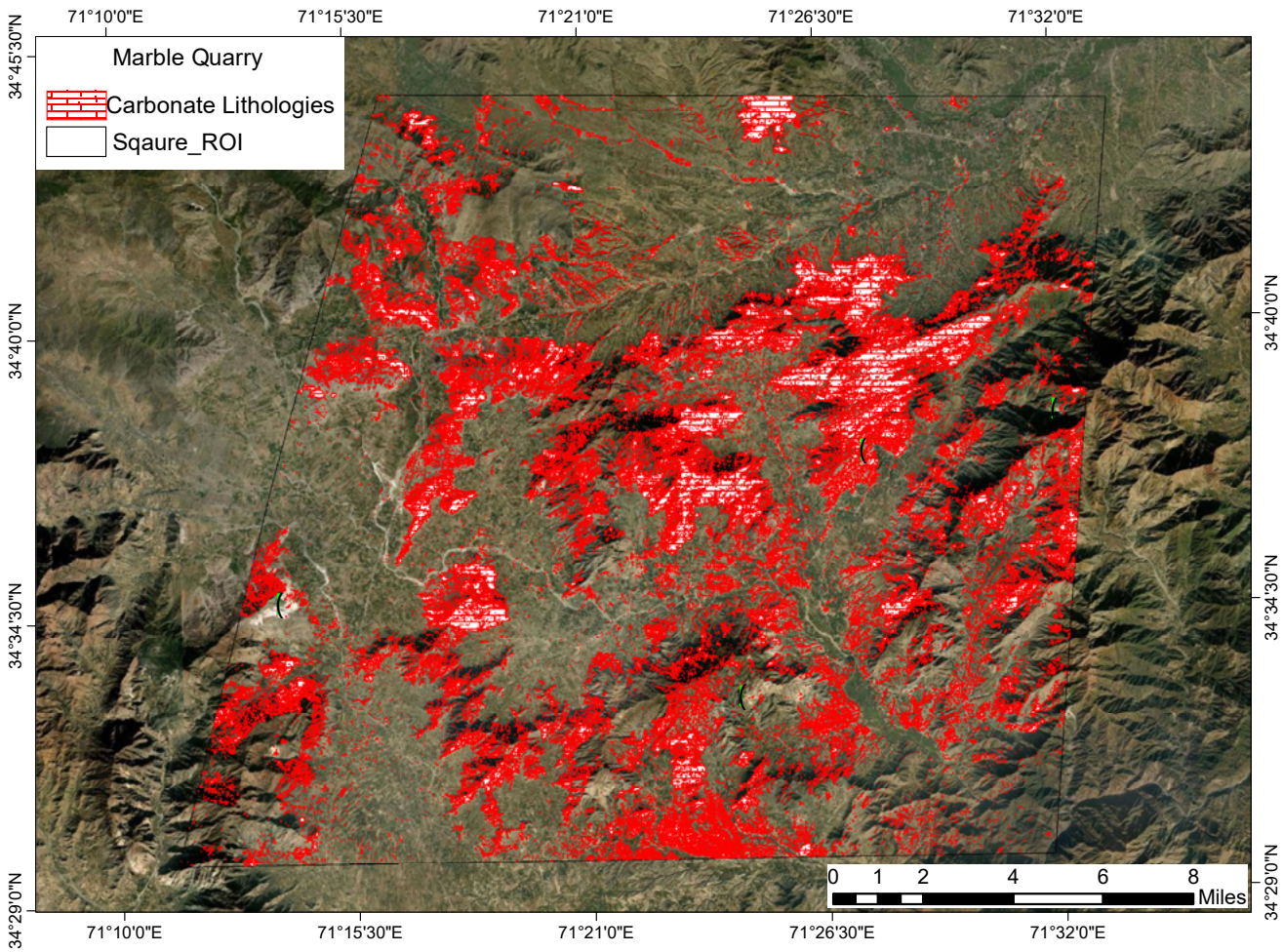

FIGURE 12. Shows the carbonate rocks exposed in the area extracted using the ASTER image and SAM classification technique. The results were visualized using Google Earth images as a base map to determine the exact locations of carbonate deposits.

as marble varieties. The results of the XRD analysis can provide valuable insights into the mineralogical composition and properties of the samples, as well as their geological history and formation conditions (Surko *et al.*, 1999). In a recent study, XRD analysis of four representative samples of marble varieties was conducted at the Mineralogy Laboratory, National Centre of Excellence in Geology. The samples were named ZM, KMM, SKM and TKM. The XRD results revealed that all four samples contained calcite ($CaCO_3$) as the major mineral. However, the analysis also revealed the presence of additional minerals in each sample. In ZM and KMM, Mg-calcite was detected, while in TKM, dolomite and ankerite were detected. The SKM sample was found to contain calcite, Mg and carlinite (Fig. 20).

DISCUSSION

This study represents the first detailed investigation of marble deposits in the north-western region of Khyber Pakhtunkhwa, previously known as the Federally Administered Tribal Area (FATA), utilizing RS technology coupled with ASTER imagery, petrographic studies, and XRD analysis. Despite the area's rich carbonate deposits, its geological potential has remained largely unexplored due to security issues and a lack of accessibility (Malkani *et al.*, 2017). The results of this study successfully identified marble quarries and carbonate deposit extinctions, marking a significant step forward in understanding the area's geology. The integration of RS techniques, specifically Environment for Visualizing Images (ENVI), Geographic Information Systems (GIS) ArcMap, and ArcScene software, allowed for the detailed mapping of lithological variations. FCC images and OIF analyses were applied to ASTER images, with band combinations b4, b6, and b8 providing the best visual results for identifying lithologies (Fig. 6). Previous studies have demonstrated the utility of ASTER imagery in similar geological settings; however, this study advances the methodology by exploring novel

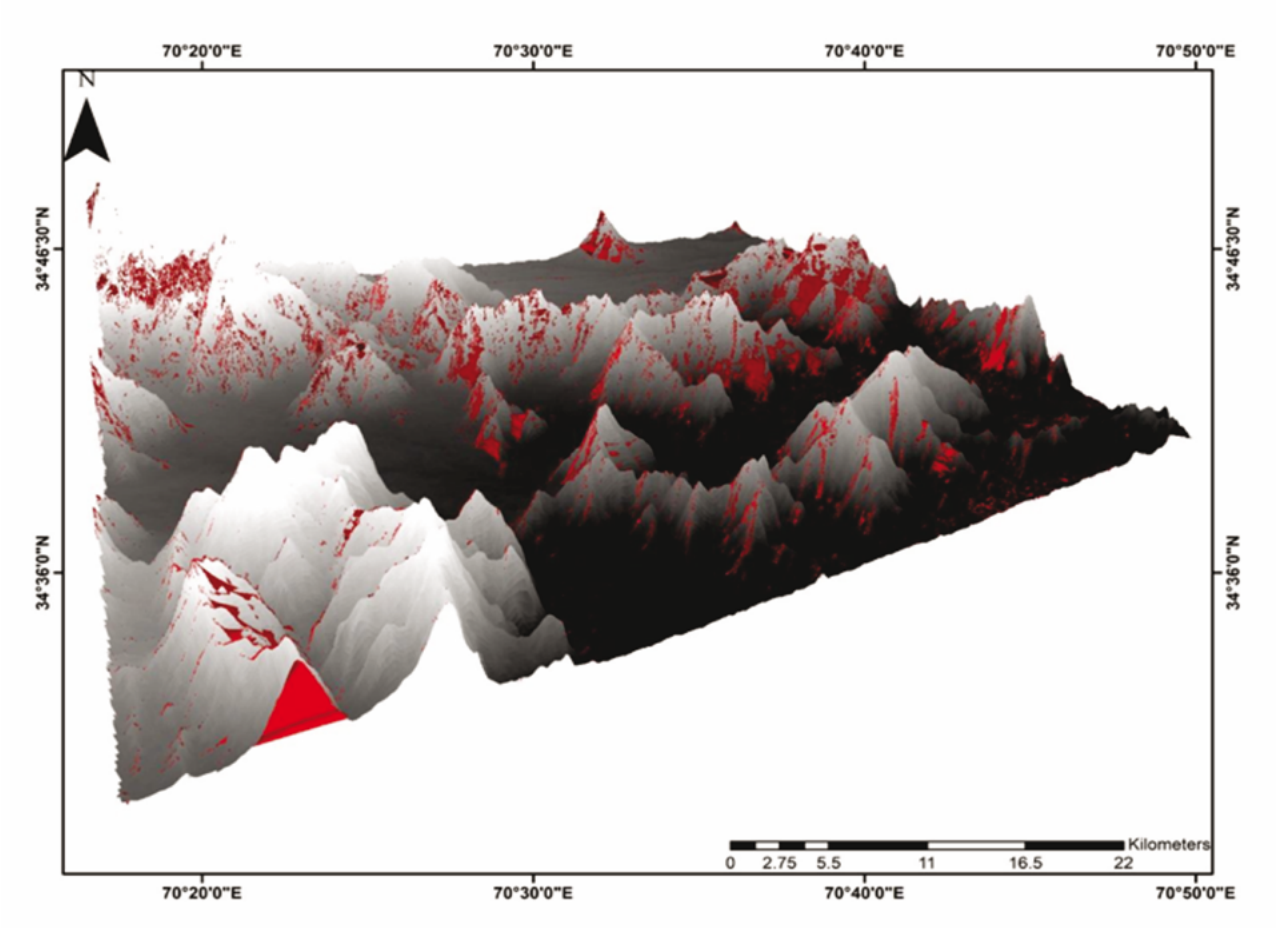

FIGURE 13. Shows the 3D model of the same area created by using GIS Arc Scene, which shows the potential zones for marble quarries.

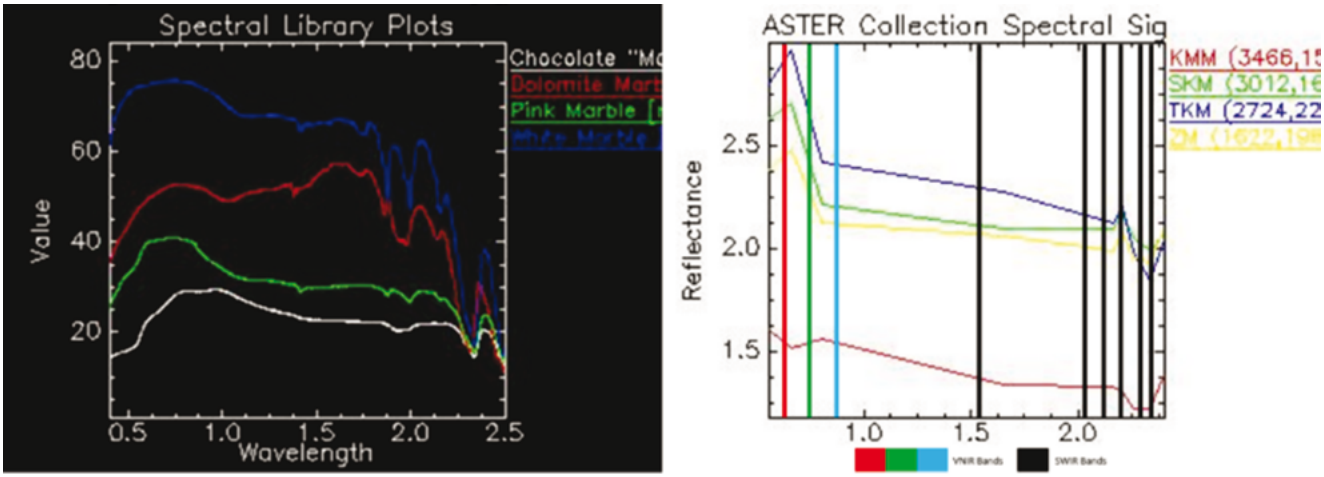

FIGURE 14. Comparison between the USGS spectral library and the spectral signature collection from the ASTER image using the ENVI library builder tool.

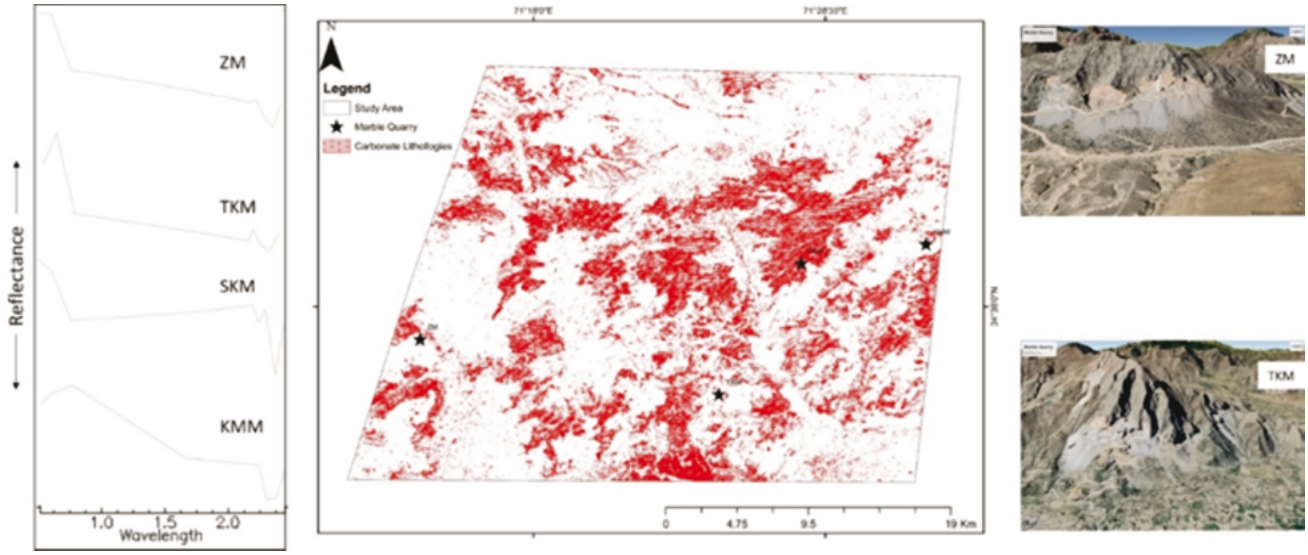

FIGURE 15. Shows the distribution of carbonate lithologies in red color, the stars highlight the spectral signature locations. and the photograph shows the quarries.

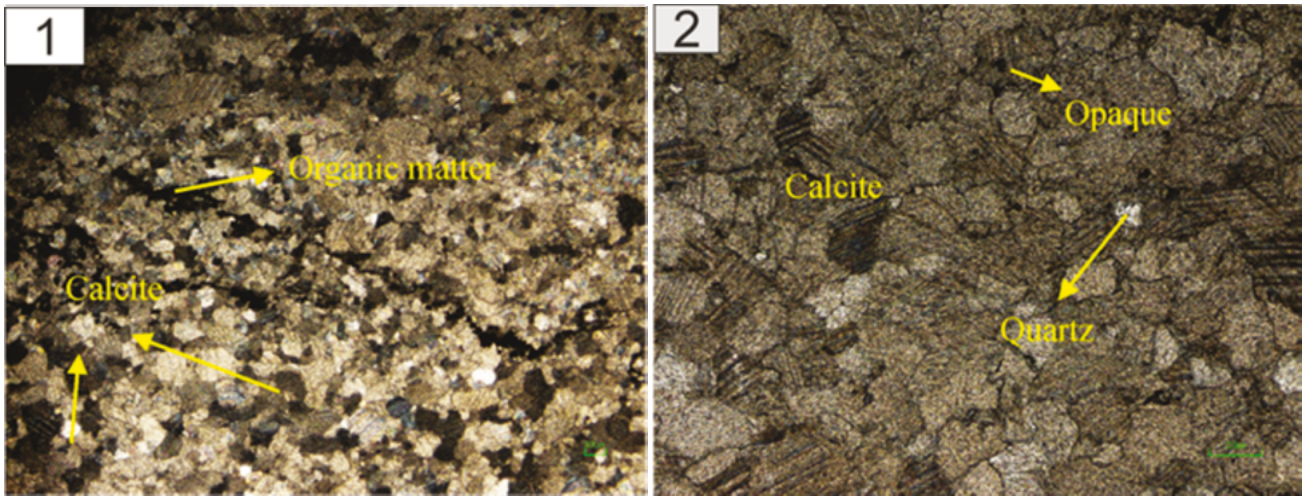

FIGURE 16. Shows calcite minerals up to 95%, quartz minerals less than 2% and rare opaque minerals.

band ratios such as BR (B7+B9)/B8, which emerged as particularly effective for detecting calcite-rich regions. This innovation aligns with existing literature but also contributes a new approach to mineral identification, enhancing the spectral differentiation of carbonate rocks. The application of PCA and Minimum Noise Fraction (MNF) analyses further strengthened the study's findings by enabling the extraction of meaningful lithological information from multispectral imagery. PCA components PC2, PC4, PC5, PC7 and PC8 were particularly effective in delineating primary lithologies, with carbonate rocks visualized in purple hues within RGB composites (Fig. 9). This capability to clearly distinguish carbonate lithologies demonstrates the robustness of PCA in areas with complex spectral signatures, reinforcing its value for future geological explorations. Similarly, MNF analysis highlighted significant lithological variation across VNIR bands MNF2 and MNF3, with carbonate rocks appearing as white and black hues in specific combinations (Fig. 10). The RGB composites derived from MNF bands, particularly MNF 246 and MNF 648, further enhanced the visualization of carbonate rocks (Fig. 11). These results confirm the effectiveness of MNF in detecting subtle lithological transitions, an observation supported by previous geological studies but expanded here by the successful application in a previously underexplored

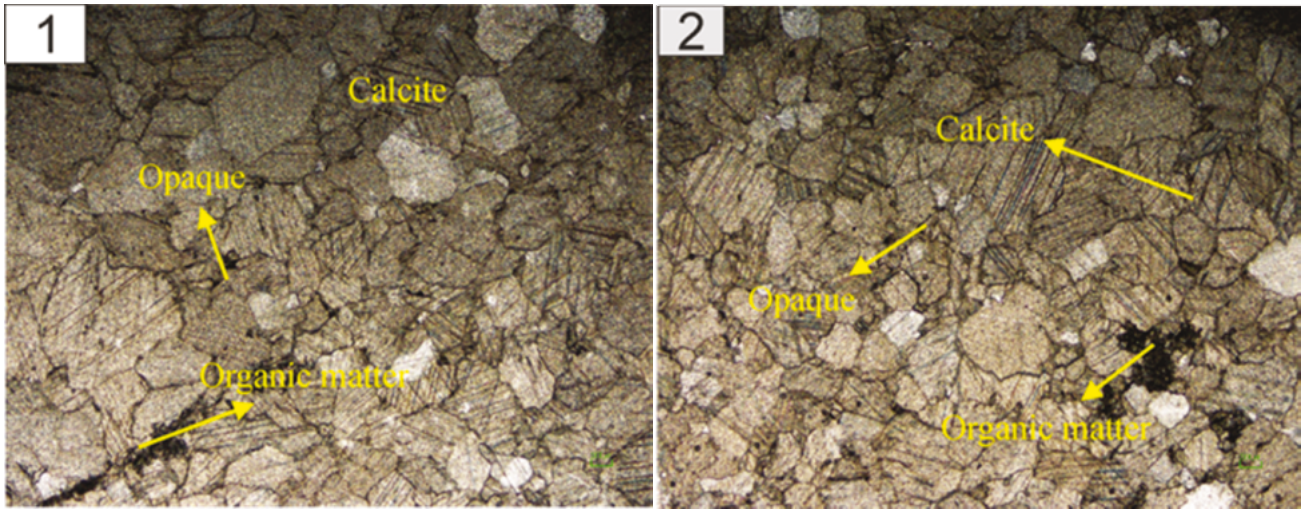

FIGURE 17. Shows that calcite minerals up to 97%, quartz minerals less than 1% and rare opaque and organic matter are also highlighted in the image.

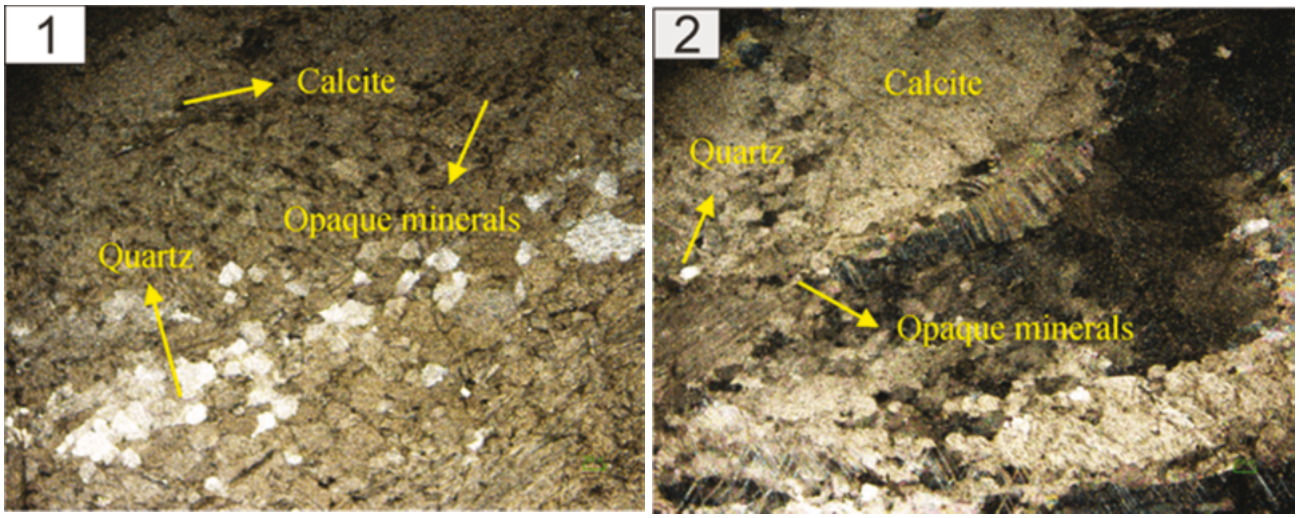

FIGURE 18. Shows calcite minerals (up to 91%), quartz minerals (up to 10%) and rare opaque minerals.

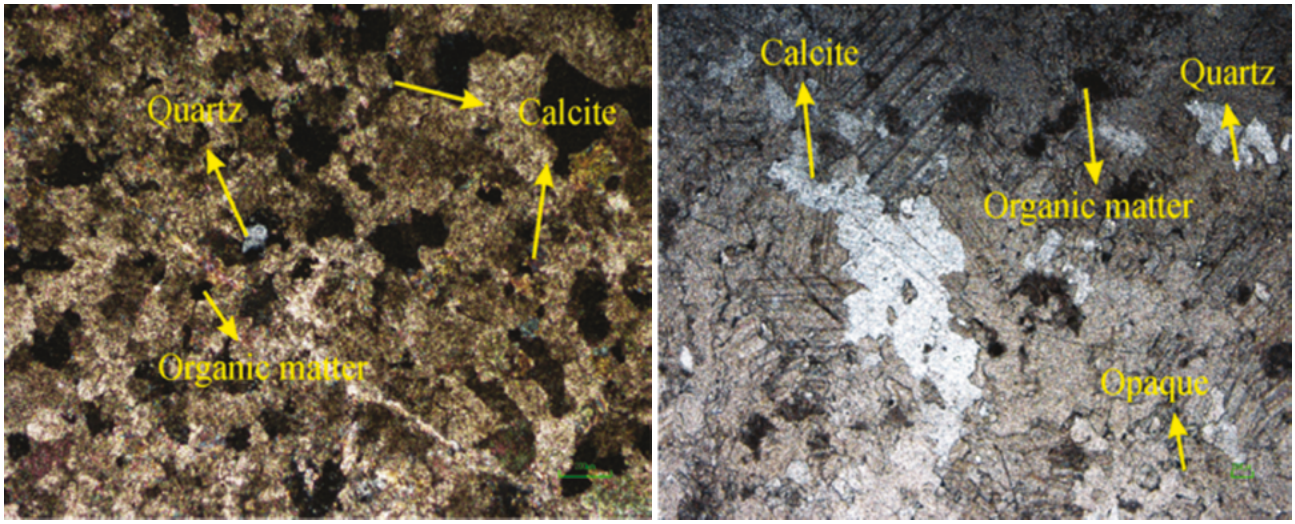

FIGURE 19. Shows calcite minerals accounting for up to 96% and organic matter from 2–4% of the Tora Howa marble quarry.

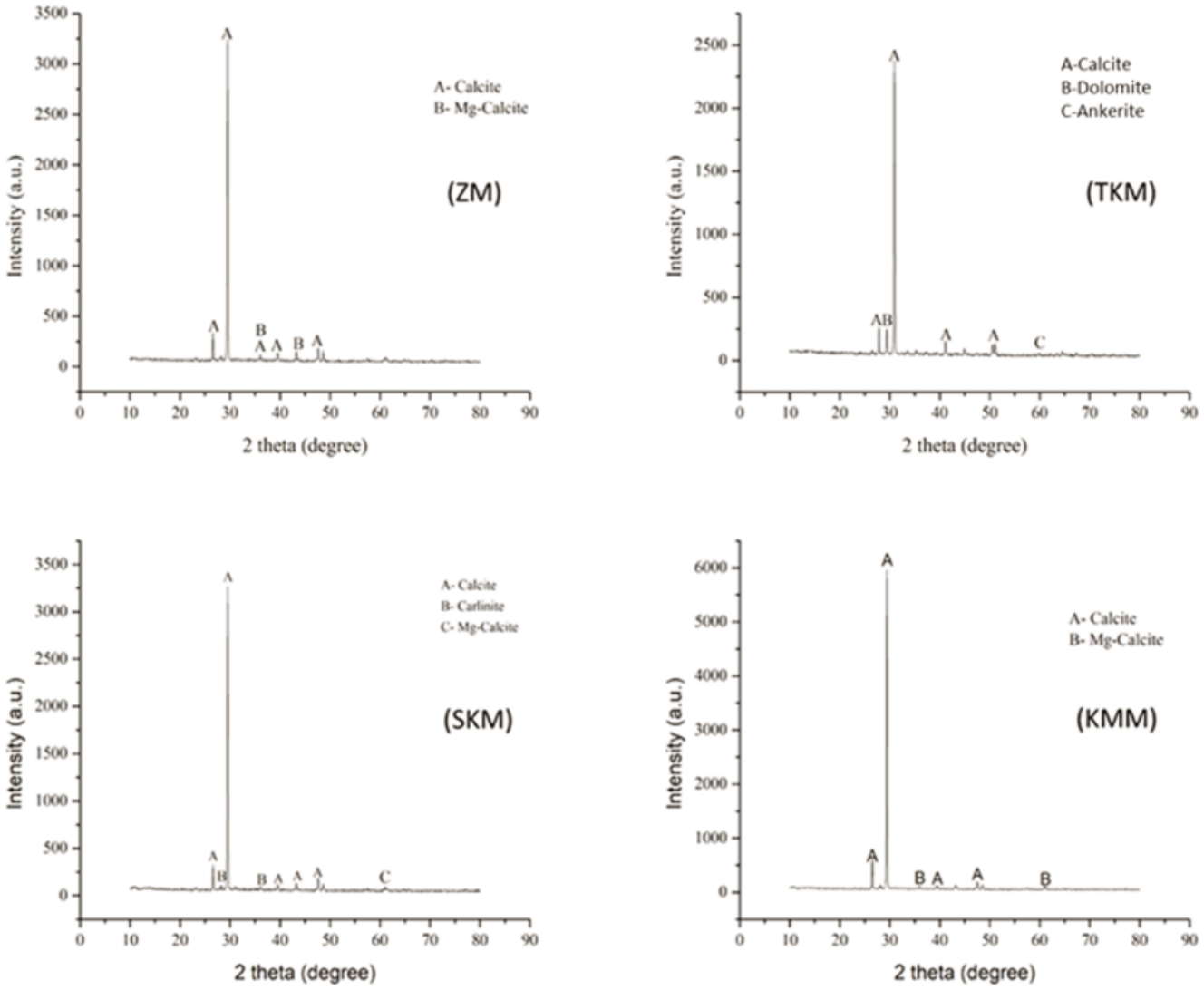

FIGURE 20. Shows the XRD results for Zm, TKM, SKM and KMM.

region. The application of the SAM technique also demonstrated precise lithological classification, allowing for the creation of detailed lithological maps of carbonate deposits (Figs. 12; 13). By comparing the collected spectra with the USGS spectral library, the study ensured high accuracy in mineral identification, a methodological approach consistent with standard practices in the field of geological remote sensing (Hegab, 2022). The results were also shown in a 3D map using GIS Arc scene software (Fig. 13). The collected spectra were compared with the USGS spectral library spectra for different types of minerals (Fig. 14). While this study provides a comprehensive geological investigation, certain limitations exist. The security and accessibility challenges that have historically hindered exploration in the region may have also limited the study's field-based validation. However, the combined use of RS technologies, petrography, and XRD analysis (Fig. 16; 17; 18; 19; 20) provided sufficient data for robust conclusions. Future research could benefit from expanding field sampling and incorporating higher-resolution RS imagery to further refine lithological classifications and improve deposit quantification.

This study's findings have significant implications for the economic development of the region, given the mapping of marble quarries. The methodological advancements made here in RS and ASTER imagery analysis can be applied to similar regions facing accessibility challenges, offering a non-invasive approach to mineral exploration. Moreover, this work has the potential to attract both local and international investment in Pakistan's mineral sector, contributing to regional economic growth and the global supply of marble and related minerals for industries.

CONCLUSION

This comprehensive investigation of marble deposits in north-western Khyber Pakhtunkhwa highlights the effectiveness of integrating RS technology, advanced spectral analysis, petrographic and mineralogical studies. Despite the region's security challenges, the study successfully identified and characterized significant carbonate deposits, revealing their geological composition and distribution. The integration of ASTER imagery with software applications like ENVI and GIS ArcMap has played a pivotal role in identifying and characterizing marble quarries and carbonate lithologies. Various spectral analysis techniques, including FCC, BR, PCA, and MNF, have enhanced the understanding of lithological variations, allowing for the identification of spectral signatures indicative of calcite-rich zones. The application of techniques such as ASTER imagery analysis, spectral classification methods, and 3D mapping has enhanced our understanding of these resources. Moreover, Petrographic studies have corroborated the findings from spectral analysis, revealing the presence of calcite and dolomite minerals with minor amounts of organic/opaque matter in various marble samples. XRD patterns confirmed the mineral composition identified through RS analysis, further validating the accuracy of remote sensing-based mineral identification techniques. Overall, this research not only enriches the geological knowledge of the region but also provides critical insights for future resource exploration and sustainable mine planning in carbonate-rich areas.

ACKNOWLEDGMENTS

The authors strongly acknowledge the GIS and Space Applications in Geosciences Laboratory - GSAG Lab, National Centre of Excellence in Geology-NCEG, University of Peshawar, Pakistan affiliated with National Centre of GIS and Space Applications (NCGSA) (Institute of Space Technology, Islamabad, Pakistan), for providing the well-equipped platform for completing this work. The authors extend their appreciation to Abdullah Alrushaid Chair for Earth Science Remote Sensing Research at King Saud university for funding.

DATA AVAILABILITY STATEMENT

All published data will be available on a request from the corresponding Author.

AUTHOR CONTRIBUTIONS

Conceptualization, M.S., methodology, M.S. and L.A.; software, M.S.; validation, M.S., L.A. and F.A.; formal analysis, M.S.; investigation, L.A. and F.A.; resources, M.S., L.A. and F.A.; data curation, L.A. and F.A.; writing—original draft preparation, M.S.; writing—review and editing, L.A. and F.A.; visualization, M.S.; supervision, L.A. and F.A.; project administration; All authors have read and agreed to the published version of the manuscript.

REFERENCES

Ahmad, S., Khan, N., 2019. Marble industry role in the socio-economic development of marble industrial owners of district Mohmand federal administered tribal area-Pakistan. Ind. Eng. Lett, 9(3), 10-7176.

Anjum, M.N., Ashfaq, M., Ullah, S., Yaseen, M., Ali, L., Prsek, J., Rehman, G., 2021. Economic geology of the carbonate rocks from Mesozoic Alpurai group, Peshawar basin, Pakistan. Iran. J. Earth Sci., 13, 239-250.

Ali, H.F, El Ata, A.A., Youssef, M.A.S., Salem, S.M., Ghoneim, S.M., 2023. A newly-developed multi-algorithm integration technique for mapping the potentially mineralized alteration zones. The Egyptian Journal of Remote Sensing and Space Science, 26(3), 691-711.

Alshehri, F., Shahab, M., Azer, M.K., Pande, C.B., Abanumay, F.A., 2025. An integrated remote sensing and geochemical approach for mapping the Kamal layered mafic intrusion in the Arabian Shield, Northwest Saudi Arabia. Environmental Earth Sciences, 84(1), 1-18.

Azizi, H., Tarverdi, M.A., Akbarpour, A., 2010. Extraction of hydrothermal alterations from ASTER SWIR data from east Zanjan, northern Iran. Adv. Space Res., 46, 99-109.

Berk, A.G., Anderson, G.P., Acharya, P.K., Chetwynd, J.H., Bernstein, L.S., Shettle, E.P., Matthew, M.W., Adler-Golden, S.M., 2009. MODTRAN4 user's manual. Air Force Res. Lab., 1, 98-107.

Bouazza, N., El Mrihi, A., Maâte, A., 2016. Geochemical Assessment of Limestone for Cement Manufacturing. Procedia Technol., 1, 22-211.

Careddu, N., Marras, G., Siotto, G., 2014. Recovery of sawdust resulting from marble processing plants for future uses in high value-added products. J. Clean. Prod., 84, 533-539.

Carranza, E.J.M., Hale, M., 2002. Where porphyry copper deposits are spatially localized? A case study in Benguet province Philippines. Nat Resour J, 11(1), 45-59.

Chen, X., Warner, T.A., Campagna, D.J., 2007. Integrating visible, near-infrared and shortwave infrared hyperspectral and multispectral thermal imagery for geological mapping at Cuprite, Nevada. Journal of Remote Sensing of Environment, 110, 344-356. DOI: https://doi.org/10.1016/j.rse.2007.03.015

Crosta, A.P., Moore, J.M., 1989. Geological mapping using Landsat thematic mapper imagery in Almeria Province South-east Spain. Int J Remote Sens, 10(3), 505-514.

Crósta, A.P., De Souza Filho, C.R., Azevedo, F., Brodie, C., 2003. Targeting key alteration minerals in epithermal deposits in Patagonia, Argentina, using ASTER imagery and principal component analysis. Int. J. Remote Sens., 24, 4233-4240.

Dawson, J.B., 1962. The geology of Oldoinyo Lengai. Bull. Volcanol. , 24, 349-387.

Desoky, H.A., Abd El-Dayem, M., Hegab, M.A.E.R., 2024. A comparative analysis to assess the efficiency of lineament extraction utilizing satellite imagery from Landsat-8, Sentinel-2B, and Sentinel-1A: A case study around suez canal zone, Egypt. Remote Sensing Applications: Society and Environment, 36, 101312.

DiPietro, J.A., Ahmad, I., Hussain, A., 2008. Cenozoic kinematic history of the Kohistan fault in the Pakistan Himalaya. Geol. Soc. Am. Bull., 120, 1428-1440.

El-Desoky, H.M., Bachri, I., El Mezayen, A.M., Abdel-Rahman, A.M., El-Awny, H., El-Gammal, A.A., ... Almadani, S., 2024. An integrated remote sensing, petrology, and field geology analyses for Neoproterozoic basement rocks in some parts of the southern Egyptian-Nubian Shield. Scientific Reports, 14(1), 14761.

Fahad, M., Iqbal, Y., Riaz, M., Ubic, R., Abrar, M., 2016. Geo-mechanical properties of marble deposits from the Nikani Ghar and Nowshera formations of the Lesser Himalaya, Northern Pakistan—A review. Himal. Geol., 37, 17-27.

Ghoneim, S.M., Ali, H.F., Abdelrahman, K., Fnais, M.S., Lala, A.M., 2024. Integrating remote sensing and geophysical data for mapping potential gold mineralization localities at Abu Marawat area, central Eastern Desert, Egypt. Scientific Reports, 14(1), 18273.

Guo, Y., Feng, N., Christopher, S.A., Kang, P., Zhan, F.B., Hong, S., 2014. Satellite remote sensing of fine particulate matter (PM 2.5) air quality over Beijing using MODIS. Int. J. Remote Sens. , 35, 6522-6544.

Hamid, K., Alvi, U., Khosa, L., Mahmood, R., Khan, S., 2012. Geochemical evaluation of limestone deposits of Pakistan. J. Himal. Earth Sci., 45, 45.

Hay, R.L., 1989. Holocene carbonatite-nephelinite tephra deposits of Oldoinyo Lengai, Tanzania. J. Volcanol. Geotherm. Res., 37, 77-91.

Hegab, M.A.E.R., 2024. A multi-disciplinary approach for uranium exploration using remote sensing and airborne gamma-ray spectrometry data in the Gebel Duwi area, Central Eastern Desert, Egypt. Scientific Reports, 14(1), 19739.

Hegab, M.A. , 2021. Remote sensing and gamma-ray spectrometry-based gold related alteration zones detection: case study (Um Balad area), North Eastern Desert, Egypt. Pure and Applied Geophysics, 178(10), 3909-3931.

Hegab, M.A.E.R., Mousa, S.E., Salem, S.M., Farag, K., GabAllah, H., 2022. Gold-related alteration zones detection at the Um Balad Area, Egyptian Eastern Desert, using remote sensing, geophysical, and GIS data analysis. Journal of African Earth Sciences, 196, 104715.

Hegab, M.A.E.R., Mousa, S.E., Salem, S.M., Moustafa, M.S., 2022. ASTER and Aerospectrometric Data Analysis for Gold Exploration: Case Study at Um Balad Area, North Eastern Desert, Egypt. Cham, Springer Nature Switzerland, International Conference of Remote Sensing and Space Sciences Applications, 49-54.

Khan, S.D., Mahmood, K., 2008. The application of remote sensing techniques to the study of ophiolites. Earth-Sci. Rev., 3, 135-143.

Khan, S.D., Mahmood, K., Casey, J.F., 2007. Mapping of Muslim Bagh ophiolite complex (Pakistan) using new remote sensing, and field data. J. Asian Earth Sci. , 30, 333-343.

Khan, M.I., Ahmad, S., Khan, A.A., 2010. Structural Style, Evolution and Hydrocarbon Prospects of the Bhittani Range, Northwest Himalayas, Pakistan. New Orleans (Louisiana), Proceedings AAPG Annual Convention and Exhibition, 1-12.

Khan, S.M., Rahman, A.U., Ali, M., Alshehri, F., Shahab, M., Ullah, S., 2024. Pixel-Based Spatio-Statistical Analysis of Landslide Probability in Humid and Seismically Active Areas of Himalaya and Hindukush. Sustainability, 16(9), 3556.

Koca, M.Y., Ozden, G., Yavuz, A.B., Kincal, C., Onargan, T., Kucuk, K., 2006. Changes in the engineering properties of marble in fire-exposed columns. Int. J. Rock Mech. Min. Sci., 43, 520-526.

Kore, S.D., Vyas, A.K., Kabeer, K.I., S. A., 2020. A brief review on sustainable utilization of marble waste in concrete. Int. J. Sustain. Eng., 13, 264-279.

Kotnise, G.H., Chennabasappa, S., 2015. Application of Remote Sensing Techniques in Identification of Lithological Rock Units in Southern Extension of Kolar Schist Belt from Chigargunta, Chittoor District, Andhra Pradesh to Maharajagadai, Krishnagiri District, Tamil Nadu. Int. J. Innov. Sci. Eng. Technol. , 2, 210-214.

Kruse, F.A., Bordman, J.W., Huntington, J.F., 2003. Comparison of airborne hyperspectral data and EO-1 Hyperion for mineral mapping. IEEE Trans. Journal of Geosci. Remote Sens., 41, 1388-1400. DOI: http://dx.doi.org/10.1109/TGRS.2003.812908

Malekzadeh, A., Karimpour, M.H., Stern, C.R., Mazaheri, S.A., 2009. Hydrothermal Alteration Mapping in SW Birjand, Iran, using the Advanced Spaceborne Thermal Emission and Reflection Radiometer (ASTER) Image processing. Journal of Applied Sciences, 9, 829-842. DOI: http://dx.doi.org/10.3923/jas.2009.829.842

Malkani, M.S., Khosa, M.H., Alyani, M.I., Khan, K., Somro, N., Zafar, T., Arif, J., Zahid, M.A., 2017. Mineral Deposits of Khyber Pakhtunkhwa and FATA, Pakistan. Lasbela Univ. J. Sci. Technol. , 6, 23-46.

Malkani, M.S., Mahmood, Z., Alyani, M.I., Siraj, M., 2017. Mineral Resources of Khyber Pakhtunkhwa and FATA, Pakistan. Geol. Surv. Pak. Inf. Release, 996, 1-61.

Moradpour, H., Rostami Paydar, G., Feizizadeh, B., Blaschke, T., Pour, A.B., Valizadeh Kamran, K., Hossain, M.S., 2022. Fusion of ASTER satellite imagery, geochemical and geology data for gold prospecting in the Astaneh granite intrusive, West Central Iran. Int J Image Data Fusion, 13(1), 71-94.

Murphy, R.J., Monteiro, S.T., Schneider, S., 2012. Evaluating classification techniques for mapping vertical geology using field-based hyperspectral sensors. IEEE trans. Geoscience and Remote Sensing, 50, 3066-3080. DOI: http://dx.doi.org/10.1109/TGRS.2011.2178419

Ninomiya, Y., Fu, B., 2016. Regional lithological mapping using ASTER-TIR data: a case study for the Tibetan Plateau and the surrounding area. Geosciences, 6, 39.

Ninomiya, Y., Fu, B., Cudahy, T.J., 2005. Detecting lithology with Advanced Spaceborne Thermal Emission and Reflection Radiometer (ASTER) multispectral thermal infrared "radiance-at-sensor" data. Remote Sens. Environ. , 99, 127-139.

Pour, A.B., Hashim, M., 2011. Identification of hydrothermal alteration minerals for exploring of porphyry copper deposit using ASTER data, SE Iran. J. Asian Earth Sci. , 42, 1309-1323.

Pour, A.B., Hashim, M., 2012. The application of ASTER remote sensing data to porphyry copper and epithermal gold deposits. Ore Geol. Rev. , 44, 1-9.

Rajendran, S., Nasir, S., 2014. Hydrothermal altered serpentinized zone and a study of Ni-magnesioferrite–magnetite–awaruite occurrences in Wadi Hibi, Northern Oman Mountain: Discrimination through ASTER mapping. Ore Geol. Rev., 62, 211-226.

Rajendran, S., Nasir, S., 2019. ASTER capability in mapping of mineral resources of arid region: A review on mapping of mineral resources of the Sultanate of Oman. Ore Geol. Rev., 108, 33-53.

Rezaei, A., Hassani, H., Moarefvand, P., Golmohammadi, A., 2019. Lithological mapping in Sangan region in Northeast Iran using ASTER satellite data and image processing methods. Geology, ecology and landscapes, 4(1), 59-70. DOI: http://dx.doi.org/10.1080/24749508.2019.1585657

Rowan, L.C., Schmidt, R.G., Mars, J.C., 2006. Distribution of hydrothermally altered rocks in the Reko Diq, Pakistan mineralized area based on spectral analysis of ASTER data. Remote Sens. Environ. , 104, 74-87.

Saif, S.A., 1971. Geological traverse through Mohmand Agency and Bajaur, NWFP West Pakistan. Geol. Bull. , 74-81.

Schott, J.R., 2007. Remote Sensing: The Image Chain Approach. Oxford University Press.

Sekandari, M., Masoumi, I., Pour, A.B., Muslim, A.M., Hossain, M.S., Misra, A., 2022. ASTER and WorldView-3 satellite data for mapping lithology and alteration minerals associated with Pb-Zn mineralization. Geocarto Int, 37(6), 1782-1812.

Surko, C.M., Gilbert, S.J., Greaves, R.G., 1999. Progress in creating low-energy positron plasmas and beams. AIP Conf. Proc., 498, 3-12.

Ullah, Z., Li, H., Khan, A., Faisal, S., Dilek, Y., Förster, M.W., … Hussain, S.A., 2022. Mineralogy and PGE geochemistry of chromitites and peridotites of the sapat complex in the indus suture zone, northern Pakistan: implications for magmatic processes in the supra-subduction zone. International Geology Review, 65(10), 1719-1744. DOI: https://doi.org/10.1080/00206814.2022.2106519

Ullah, Z., Khan, A., Faisal, S., Zafar, T., Li, H., Farhan, M., 2022. Petrogenesis of peridotites in the Dargai Complex ophiolite, Indus Suture Zone, Northern Pakistan: Implications for two stages of melting, depletion, and enrichment of the Neo-Tethyan mantle. Lithos, 426, 106798.

Ur Rehman, A., Ahmed, W., Azam, S., Sajid, M., 2022. Characterization and thermal behavior of marble from northwestern Pakistan. Innov. Infrastruct. Solut., 7, 1-8.

Vagenas, N.V., Gatsouli, A., Kontoyannis, C.G., 2003. Quantitative analysis of synthetic calcium carbonate polymorphs using FT-IR spectroscopy. Talanta, 59, 831-836.

von Eckermann, H., 1948. The Alkaline District of Alnö Island (Alnö Alkalina Område). Esselte, 182.

Vuorinen, J.H., 2005. The Alnö Alkaline and Carbonatitic Complex, East Central Sweden: A Petrogenetic Study. Department of Geology and Geochemistry, Stockholm University.

Woolley, A.R., Barr, M.W.C., Din, V.K., Jones, G.C., Wall, F., Williams, C.T., 1991. Extrusive carbonatites from the Uyaynah area, United Arab Emirates. J. Petrol., 32, 1143-1167.

Xiong, Y., Khan, S.D., Mahmood, K., Sisson, V.B., 2011. Lithological mapping of Bela ophiolite with remote-sensing data. Int. J. Remote Sens. , 32, 41-58.

Yuan, J., Niu, Z., 2008. Evaluation of atmospheric correction using FLAASH. Earth Observation and Remote Sensing Applications, vol, 1-6.

Manuscript received July 2024;
revision accepted January 2025;
published Online February 2025.